Equation of State and Thermodynamic Properties of Pure Toluene and Dilute Aqueous Toluene Solutions in the Critical and Supercritical Regions

S. B. Kiselev* and J. F. Ely

Chemical Engineering Department, Colorado School of Mines, Golden, Colorado 80401-1887

M. Abdulagatov and A. R. Bazaev

Institute for Geothermal Problems of the Dagestan Scientific Center of the Russian Academy of Sciences, Shamilya Avenue 39A, Makhachkala 367030, Dagestan, Russia

J. W. Magee

Physical and Chemical Properties Division, National Institute of Standards and Technology, Boulder, Colorado 80305-3328

In this paper, we report new *PVTx* measurements for water + toluene binary mixtures at 11 near-critical and supercritical isotherms T = 623, 627, 629, 631, 633, 643, 645, 647, 649, 651, and 673 K and pressures up to 39 MPa at a fixed concentration of x = 0.0287 mole fraction of toluene. Using these *PVTx* data together with data obtained earlier by other authors, we developed a crossover Helmholtz free-energy model (CREOS) for pure toluene and dilute aqueous toluene solutions in a wide range of the parameters of state around the vapor−liquid critical points. In the temperature range 593 K ≤ T ≤ 680 K and density range 100 kg·m^{-3} ≤ ρ ≤ 500 kg·m^{-3}, the CREOS reproduces the *PVT* data for pure toluene with an average absolute deviation (AAD) of about 0.5%, the C_P data with an AAD of about 1%, and the sound velocity data with an AAD of about 2.6%. In water + toluene mixtures, the CREOS yields an adequate description of all available experimental data in the region bounded by $0.35\rho_c(x) \le \rho \le 1.65\rho_c(x)$ and $0.98T_c(x) \le T \le 1.15T_c(x)$ at $x \le 0.04$ mole fraction of toluene. The possibility of extrapolating the CREOS model to lower temperatures, $0.93T_c \le T \le T_c$, and higher densities and concentrations, up to $\rho = 2\rho_c$ and x = 0.12, is also discussed.

1. Introduction

The thermodynamic behavior of dilute mixtures in the vicinity of a solvent's critical point is of considerable practical and theoretical importance. Similar to carbon dioxide, supercritical water (SCW) has been proposed as an environmentally acceptable solvent and reaction medium for a number of technological applications. The thermodynamic properties of hydrocarbons in water at high temperatures and high pressures are also of considerable interest in geochemistry, petrochemistry, and organic chemistry (hydrothermal synthesis, formation of petroleum, reservoir fluids, enhanced oil recovery-in tertiary oil recovery), environmental protection (removal of hydrocarbons from wastewater and the fate of hydrocarbons in geological fluids), and new separation techniques and biological degradation without char formation.[1−6] SCW is also widely used for the extraction and destruction of organic fluids such as chemical warfare agents.[7] Design and control of the systems for supercritical fluid extraction require pure-component and mixture thermodynamic properties and molecular-based understanding of the mechanism underlying the supercritical solubility enhancement. Efficiencies of technologically important applications of SCW might be substantially improved through a better understanding of the solvation structure around the solute dissolved in SCW[8−16] and specifics of behavior of the water + hydrocarbon mixtures near the critical point of pure water. A realization of the potential of supercritical fluid solubility will prove to be impossible without a better knowledge of the thermodynamic properties of fluid mixtures near the solvent (pure water) critical point, which requires a fundamental equation of state (EOS) for pure water and dilute aqueous solutions in the critical region.

To formulate the thermodynamic properties of binary mixtures far away from the critical point, an array of analytical models and equations of state (EOSs) are usually used.[17,18] However, it is well-known that all of these analytical−classical models fail to reproduce the thermodynamic surface of pure fluids and binary mixtures in the critical region. The thermodynamic surface of a pure fluid exhibits a singularity at the critical point that can be described in terms of scaling laws with universal critical exponents and universal scaled functions.[19,20] The thermodynamic surface of a binary mixture in the critical region differs substantially from those observed in pure fluids. In the critical region, a mixture displays a regime of pure fluid-like behavior

* To whom correspondence should be addressed: Phone: (303) 273-3190. Fax: (303) 273-3730. E-mail: skiselev@mines.edu.

10.1021/ie010307m CCC: $22.00
Published on Web 09/20/2001

at a fixed field variable (chemical potential $\tilde{\mu}$) rather than at a fixed composition x.[21−23] As a consequence, all thermodynamic properties calculated at fixed composition are renormalized in the critical region of a binary mixture.[20,24,25]

There are few crossover models of mixtures formulated in terms of the chemical potential that incorporate scaling laws in the critical region and transform into an analytical EOS far away from the critical region. Examples include the six-term crossover model developed by Sengers and co-workers,[26−28] the crossover Leung−Griffiths model developed by Belyakov et al.,[29,30] and the more extensive parametric crossover model developed by Kiselev and Rainwater.[31] The Helmholtz free energy in the latter model was represented in a universal parametric form, which does not depend on the details of the intermolecular interaction and is equally valid for any pure fluid and binary mixture in the critical region, including ionic and aqueous solutions. All system-dependent parameters of this model are expressed as functions of the excess critical compressibility factor of the mixture. Therefore, if the critical locus of the mixture is known, all other thermodynamic properties can be predicted. So far, the computer program CREOS97, based on the parametric crossover model developed by Kiselev and Rainwater,[31] has been successfully applied to the prediction of the vapor−liquid equilibrium (VLE) surface and thermodynamic properties for more than 20 binary mixtures.[30−33] However, most of these applications were restricted to type I binary mixtures, according to the Van Konynenberg−Scott specification,[34] and the question of the application of the theoretical crossover models to other types of binary mixtures remains open. Few attempts were made to extend the nonclassical crossover approach to the binary mixtures near the liquid−liquid critical points,[35] types V[36] and II[37] binary mixtures. However, so far, no practical crossover model capable of reproducing the thermodynamic surface for all five types of binary mixtures has been developed.

In this work, we applied the parametric crossover model incorporated in the program CREOS97 to the description of the phase behavior and thermodynamic properties of critical dilute aqueous toluene mixtures, which, according to the Van Konynenberg−Scott specification, correspond to the type III mixture. To identify the $T_c(x)$ and $\rho_c(x)$ critical locus as $x \rightarrow 0$, we have measured the $PVTx$ properties of dilute water + toluene mixtures in the vicinity of the critical point of pure water. These data together with $PVTx$ data reported by Degrange[38] have been used to develop a crossover EOS for water + toluene mixtures in the wide region around the critical point of pure water. We proceed as follows. In section 2 we describe the parametric crossover model for binary mixtures. In section 3 we give a detailed review of the existing experimental data for the dilute critical water + toluene mixtures. Our original experimental measurements are presented in section 4. In section 5 we describe the crossover EOS for pure toluene and dilute aqueous toluene solutions. Comparisons with experimental data for pure toluene and water + toluene mixtures are discussed in section 6. Our results are summarized in section 7.

2. Crossover Free-Energy Model

A phenomenological procedure for dealing with the crossover behavior of the Helmhotz free-energy density in the critical region of pure fluids has been developed by Kiselev and co-workers.[39−41] Later, using the critical point universality (also called the isomorphism principle[20,24]), Kiselev[42] extended this crossover approach to binary mixtures. In the present paper, for the prediction of the thermodynamic properties and the phase behavior of water + toluene mixtures in and beyond the critical region, we use the parametric crossover model developed by Kiselev,[42] as modified by Kiselev and Rainwater.[31,32] The crossover free-energy density in this model is given by

$$\rho\tilde{A}(T,\rho,\tilde{x}) = \rho A(T,\rho,x) - \rho\tilde{\mu}(T,\rho,x) \tag{1}$$

where $\tilde{\mu} = \mu_2 - \mu_1$ is the difference of the chemical potentials μ_1 and μ_2 of the mixture components, $x = N_2/(N_1 + N_2)$ is the mole fraction of the second component in the mixture, $\rho A(T,\rho,x)$ is the Helmholtz free-energy density of the mixture, and the isomorphic variable $\tilde{x}$ is related to the field variable ζ, first introduced by Leung and Griffiths,[43] by the relation

$$\tilde{x} = \frac{e^{\tilde{\mu}/RT}}{1 + e^{\tilde{\mu}/RT}} = 1 - \zeta \tag{2}$$

The thermodynamic equation

$$x = -\tilde{x}(1 - \tilde{x})\left(\frac{\partial\tilde{A}}{\partial\tilde{x}}\right)_{T,\rho}\frac{1}{RT} \tag{3}$$

(where R is the universal gas constant) provides a relation between the concentration x and the isomorphic variable $\tilde{x}$. Similar to the concentration, the isomorphic variable $\tilde{x}$ changes from 0 to 1 for $0 \le x \le 1$. At fixed $\tilde{x}$, the isomorphic free energy $\rho\tilde{A}$ is the same function of T and ρ as the Helmholtz free-energy density of a one-component fluid[39−42]

$$\frac{\rho\tilde{A}(T,\rho,\tilde{x})}{RT_{c0}\rho_{c0}} = \tilde{k}r^{2-\alpha}\tilde{R}^{\alpha}(q)\,[\tilde{a}\Psi_0(\vartheta) + \sum_{i=1}^{5}\tilde{c}_i r^{\Delta_i}\tilde{R}^{-\tilde{\Delta}_i}(q)\,\Psi_i(\vartheta)] + \sum_{i=1}^{4}\left(\tilde{A}_i + \frac{\rho}{\rho_c(\tilde{x})}\tilde{m}_i\right)\tau^i(\tilde{x}) - \frac{P_c(\tilde{x})}{RT_{c0}\rho_{c0}} + \frac{\rho T}{T_{c0}\rho_{c0}}[\ln(1 - \tilde{x}) + \tilde{m}_0] \tag{4}$$

$$\tau = \frac{T - T_c(\tilde{x})}{T_c(\tilde{x})} = r(1 - b^2\vartheta) \tag{5}$$

$$\Delta\rho = \frac{\rho - \rho_c(\tilde{x})}{\rho_c(\tilde{x})} = \tilde{k}r^{\beta}\tilde{R}^{-\beta+1/2}(q)\,\vartheta + \tilde{d}_1\tau \tag{6}$$

where b^2 is a universal linear-model parameter[42] and $\tilde{k}$, $\tilde{d}_1$, $\tilde{a}$, and $\tilde{c}_i$ are system-dependent coefficients. The scaled functions $\Psi_i(\vartheta)$ are the universal analytical functions of the parametric variable ϑ

$$\Psi_i(\vartheta) = \sum_{j=0}^{5}\alpha_{ij}\vartheta^j \quad (i = 0, 1, ..., 5) \tag{7}$$

Table 1. Universal Scaled Functions

$$\Psi_0(\vartheta) = \frac{1}{2b^4}\left[\frac{2\beta(b^2-1)}{2-\alpha} + \frac{2\beta(2\gamma-1)}{\gamma(1-\alpha)}(1-b^2\vartheta^2) - \frac{(1-2\beta)}{\alpha}(1-b^2\vartheta^2)^2\right]$$

$$\Psi_1(\vartheta) = \frac{1}{2b^2(1-\alpha+\Delta_1)}\left[\frac{\gamma+\Delta_1}{2-\alpha+\Delta_1} - (1-2\beta)b^2\vartheta^2\right]$$

$$\Psi_2(\vartheta) = \frac{1}{2b^2(1-\alpha+\Delta_2)}\left[\frac{\gamma+\Delta_2}{2-\alpha+\Delta_2} - (1-2\beta)b^2\vartheta^2\right]$$

$$\Psi_3(\vartheta) = \vartheta - \frac{2}{3}(e_0-\beta)b^2\vartheta^3 + \frac{e_1(1-2\beta)}{5-2e_0}b^4\vartheta^5$$

$$\Psi_4(\vartheta) = \frac{1}{3}b^2\vartheta^3 - \frac{e_2(1-2\beta)}{5-2e_0}b^4\vartheta^5$$

$$\Psi_5(\vartheta) = \frac{1}{3}b^2\vartheta^3 - \frac{e_4(1-2\beta)}{2e_3-5}b^4\vartheta^5$$

The exact expressions for these functions are given in Table 1. The crossover function $\tilde{R}(q)$ is defined by the expression[31]

$$\tilde{R}(q) = \left(1 + \frac{q^{2\Delta_0}}{1+q^{\Delta_0}}\right)^{1/\Delta_0}, \quad q = r\tilde{g} \tag{8}$$

The system-dependent parameter $\tilde{g} \propto Gi^{-1}$, where Gi is the Ginzburg number for the fluid of interest[44−46] and Δ_0 is a universal constant. In eqs 4−8, all nonuniversal parameters as well as the critical parameters $T_c(\tilde{x})$, $\rho_c(\tilde{x})$, and $P_c(\tilde{x})$ are analytic functions of the isomorphic variable $\tilde{x}$. In previous work[31−33,47,48] for type I binary mixtures, these functions were represented as simple polynomial forms of $\tilde{x}$ and $1-\tilde{x}$. The water + toluene system corresponds to a type III mixture, in which the VLE critical locus at high pressures is transformed into the liquid−liquid equilibrium (LLE) critical locus that is disconnected from the critical point of the pure solute−toluene (see Figure 1). Therefore, for $T_c(\tilde{x})$ and $\rho_c(\tilde{x})$ in dilute water + toluene solutions ($x \le 0.15$), we use here the same expressions as those in previous papers[31,32,42]

$$T_c(\tilde{x}) = T_{c0}(1-\tilde{x}) + T_{c1}\tilde{x} + (1-\tilde{x})\sum_{i=1} T_i x^i \tag{9}$$

$$\rho_c(\tilde{x}) = \rho_{c0}(1-\tilde{x}) + \rho_{c1}\tilde{x} + (1-\tilde{x})\sum_{i=1} \rho_i x^i \tag{10}$$

while the critical pressure is expressed as a function of $T_c(\tilde{x})$

$$P_c(\tilde{x}) = \begin{cases} P_{c0} + \sum_{i=1} P_i[T_c(\tilde{x}) - T_{c0}]^i, & T^c_{\min} < T_c(\tilde{x}) \le T_{c0} \\ P_{c1}, & \tilde{x} = 1 \end{cases} \tag{11}$$

where $T^c_{\min}$ is the lowest critical temperature at $P_c - T_c$ critical locus (see Figure 1) and the subscripts c0 and c1 correspond to the pure solvent (water) and solute (toluene), respectively.

In addition to eqs 9−11, we also adopted a so-called critical line condition (CLC), which implies that a zero level of the entropy of a binary mixture can be chosen so that the isomorphic variable $\tilde{x} = x$ along the whole critical line, including the pure solvent limit. The CLC applied here is similar to the CLC implemented earlier by Kiselev et al.[31,32,42] for type I mixtures

$$\frac{d\tilde{m}_0}{d\tilde{x}} = \frac{1}{RT_c\rho_c}\frac{dP_c}{d\tilde{x}} + (\tilde{A}_1 + \tilde{m}_1)\frac{\rho_{c0}}{\rho_c}\frac{T_{c0}}{T_c^2}\frac{dT_c}{d\tilde{x}} \tag{12}$$

To specify the crossover equation for $\tilde{A}(T,\rho,\tilde{x})$ of a binary mixture, we also need the system-dependent parameters $\tilde{d}_1(\tilde{x})$, $\tilde{k}(\tilde{x})$, $\tilde{a}(\tilde{x})$, $\tilde{c}_i(\tilde{x})$, $\tilde{m}_i(\tilde{x})$, and $\tilde{A}_i(\tilde{x})$ as functions of the isomorphic variable $\tilde{x}$. To represent all system-dependent parameters in eqs 4−8, designated as $\tilde{k}_i(\tilde{x})$, as functions of $\tilde{x}$, we utilize the hypothesis[49] that in binary mixtures all system-dependent parameters depend on $\tilde{x}$ only through the excess critical compressibility factor $\Delta Z_c(\tilde{x})$, where

$$\Delta Z_c(\tilde{x}) = Z_c(\tilde{x}) - Z_{cid}(\tilde{x}) \tag{13}$$

is the difference between the actual compressibility factor of a mixture $Z_c(\tilde{x}) = P_c(\tilde{x})/R\rho_c(\tilde{x})\ T_c(\tilde{x})$ and its "ideal" part $Z_{cid}(\tilde{x}) = Z_{c0}(\tilde{x})\ (1-\tilde{x}) - Z_{c1}\tilde{x}$. The dimensionless coefficients $\tilde{d}_1(\tilde{x})$ and $\tilde{k}(\tilde{x})$ are written in the form[31,42]

$$\tilde{k}_i(\tilde{x}) = k_{i0} + (k_{i1} - k_{i0})\tilde{x} + k_i^{(1)}\Delta Z_c(\tilde{x}) + k_i^{(2)}\Delta Z_c(\tilde{x})^2 \tag{14}$$

and all other coefficients are given by

$$\tilde{k}_i(\tilde{x}) = \frac{P_c(\tilde{x})}{R\rho_c(\tilde{x})\ T_c(\tilde{x})}[k_{i0} + (k_{i1} - k_{i0})\tilde{x} + k_i^{(1)}\Delta Z_c(\tilde{x}) + k_i^{(2)}\Delta Z_c(\tilde{x})^2] \tag{15}$$

Within the law of corresponding states (LCS), the mixing coefficients $k_i^{(j)}$ in eqs 14 and 15 are universal constants for all type I binary mixtures with $\Delta Z_c \le 0.2$.[31]

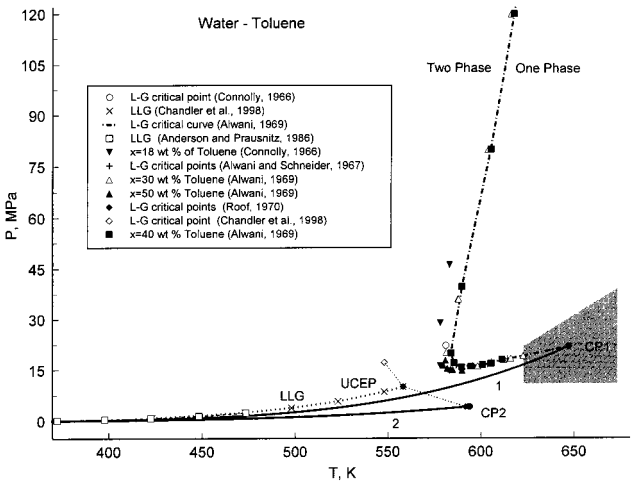

Figure 1. Pressure−temperature phase diagram for the water + toluene mixture. The symbols with the dotted eye guide lines represent experimental data:[81−84,86] CP1, critical point of pure water; CP2, critical point of pure toluene. The dash-dotted line represents the critical locus by Alwani and Schneider.[87] The solid lines represent the following: 1, vapor-pressure curve calculated with the IAPWS-95 formulation for water;[94] 2, vapor-pressure curve calculated with the multiparametric EOS of Lemmon and Jacobsen.[80] The shaded area represents the region where the new *PVTx* data have been obtained.

Table 2. Universal Constants

$\alpha = 0.110$	$\tilde{\Delta}_3 = \tilde{\Delta}_4 = \Delta_3 - 0.5 = 0.065$
$\beta = 0.325$	$\tilde{\Delta}_5 = \Delta_5 - 0.5 = 0.69$
$\gamma = 2 - \alpha - 2\beta = 1.24$	$e_0 = 2\gamma + 3\beta - 1 = 2.455$
$b^2 = (\lambda - 2\beta)/\gamma(1 - 2\beta) \cong 1.359$	$e_1 = (5 - 2e_0)(e_0 - \beta)(2e_0 - 3)/3(e_0 - 5\beta) \cong 0.147$
$\Delta_1 = \tilde{\Delta}_1 = 0.51$	$e_2 = (5 - 2e_0)(e_0 - 3\beta)/3(e_0 - 5\beta) \cong 5.35 \cdot 10^{-2}$
$\Delta_2 = \tilde{\Delta}_2 = 2\Delta_1 = 1.02$	$e_3 = 2 - \alpha - \Delta_5 = 3.08$
$\Delta_3 = \Delta_4 = \gamma + \beta - 1 = 0.565$	$e_4 = (2e_3 - 5)(e_3 - 3\beta)/3(e_3 - 5\beta) \cong 0.559$
$\Delta_5 = 1.19$	$\Delta_0 = 0.5$

The parametric crossover model for binary mixtures is specified by eqs 4−15 and contains the following universal constants: the critical exponents α, β, Δ_i, and $\tilde{\Delta}_i$ and the linear-model parameter b^2. The values of all universal constants are listed in Table 2.

3. Available Experimental Data

3.1. Pure Toluene. The *PVT* properties of pure toluene have been studied by a number of authors.[50−63] Most of these measurements were performed at temperatures up to 450 K except for the measurements of Straty et al.,[59] Akhundov and Abdullaev,[60,63] and Franck et al.,[62] where the measurements were made at temperatures up to 673 K and at pressures up to 300 MPa. Akhundov and Abdullaev[63] presented very extensive experimental *PVT* data for toluene in the temperature range from 573 to 673 K at pressures up to 50 MPa. The uncertainty of these data is 0.05% for densities above 1000 kg·m^{-3} and about 0.1% for densities lower than 1000 kg·m^{-3}. Measurements have been made using two piezometers with different volumes of 125 and 890 cm^3. The differences between the measurements are 0.01−0.02%. The pressure was measured with deadweight pressure gauges MP-600 (at high pressures) and MP-60 (at low pressures) with an uncertainty of 0.01%. The sample had a purity of 99.98 mass %. Akhundov and Abdullaev[60] reported *PVT* measurements for toluene along 13 near-critical isotherms between 591.15 and 603.15 K, densities from 275.00 to 359.51 kg·m^{-3}, and pressures between 4.2 and 4.9 MPa. The five isotherms 592.15, 593.15, 593.95, 598.15, and 603.15 K were measured twice to test the reproducibility of the measurements. The differences between the test measurements are 0.02−0.03%. The pressure was measured using the MP-60 with an uncertainty of ±0.02%. The uncertainty of the density measurements is about ±0.02 to ±0.03%. From the *PVT* measurements, the following critical parameters were extracted: $T_c = 593.85$ K, $P_c = 4.2358$ MPa, and $\rho_c = 289.77 \pm 3$ kg·m^{-3}. The data presented by Straty et al.[59] cover the temperature range between 348 and 673 K at pressures up to 35 MPa. They measured 27 pseudoisochores from 156.6 and 829.2 kg·m^{-3}. Except for the critical region, the estimated uncertainty of density measurements is 0.2% at the highest densities and 0.35% at the lowest densities. The agreement between the Akhundov and Abdullaev[60,63] data and the Straty et al.[59] data is about 0.4%, except in the critical region where the density differences reached about 1.5%. The maximum deviations are about 1.2−1.9% along the isotherm 623.15 K at densities between 285.6 and 534.4 kg·m^{-3}. In general, there is excellent consistency between the Akhundov and Abdullaev[60,63] data and the Straty et al.[59] data. These data are recommended for inclusion in the experimental base for developing an EOS. The density of toluene has been measured from 323 to 673 K and between 5 and 300 MPa by Franck et al.[62] along 16 isochores with densities from 335 to 950 kg·m^{-3}. Their measurements were made using a cylindrical autoclave with an internal volume of 66.3 cm^3. These data show good agreement (within 0.2%) with the data by Magee and Bruno[58] and Pöhler and Kiran[61] at temperatures up to 423 K and pressures up to 50 MPa. The differences between the Franck et al.[62] data and measurements by Akhundov and Abdullaev[60,63] and Straty et al.[59] at high temperatures and low pressures (P < 50 MPa) reach 1.5%. Magee and Bruno[58] reported data in the temperature range from 180 to 400 K and at pressures up to 35 MPa. Measurements were carried out on 20 liquid isochores between 791 and 973 kg·m^{-3}. The pressure was measured with an uncertainty of 0.01% at P > 3 MPa and 0.05% at P < 3 MPa. The uncertainty of density measurements is 0.05%. Measurements were made using a nearly constant volume container with an internal volume of 28.5193 ± 0.003 cm^3. These data show good agreement (within 0.2%) with the data derived by Akhundov and Abdullaev,[60,63] Kashiwagi et al.,[53] and Muringer et al.[55] Excellent agreement within 0.05% is observed between the Magee and Bruno[58] and Straty et al.[59] data. A Kay-type apparatus was used to measure the *PVT* of gaseous toluene from about 423 to 498 K by Marcos et al.[54] The values of the second virial coefficients were calculated for the measured isotherms 423.26, 448.13, 473.19, and 498.29 K.

Saturated densities for toluene were reported by Polikhronidi et al.[64] from calorimetric C_V measurements, Mamedov and Akhundov,[65] Magee and Bruno,[58] Zotov et al.,[66] Okhotin et al.,[67] Hales and Townsend,[68] Chirico and Steele,[69] Rudenko et al.,[70] Shraiber and Pechenyuk,[71] and Francis.[72] There is satisfactory agreement (within 2%) between the data reported by Polikhronidi et al.[64] and the data reported by Mamedov and Akhundov.[65] In the range far from the critical point ($T \leq 588$ K), the Polikhronidi et al.[64] results for the saturated liquid densities show good agreement (within about ±1%) with the corresponding experimental data presented in refs 58 and 65−71. At high densities and at temperatures below 525 K, the agreement between all of these data sets is excellent (AAD = 0.3%). The saturated liquid data in the critical region by Mamedov and Akhundov[65] show deviations within 2% of data by Polikhronidi et al.,[64] and the saturated vapor densities deviate by about 3%. The values of the saturated liquid densities calculated from the Goodwin[73] EOS show deviations from the data by Polikhronidi et al.[64] of 2−3% in the immediate vicinity of the critical point (about 1 K around the critical temperature). At temperatures below 592 K, the deviations are about 1.5%, while for vapor isochores in the immediate vicinity of the critical point (about 1−2 K around the critical temperature), the deviations of densities calculated from the Goodwin[73] EOS are between 5% and 7%. The reason for this is that Goodwin[73] calculated the saturated vapor densities ρ_S'' from the thermodynamic relation (Clapeyron equation)

using the experimental saturated liquid densities ρ'_S, vapor pressures $P_S(T)$, and enthalpies of vaporization ΔH_{vap}. Because of propagated uncertainties, values derived from eq 16 can be less accurate than direct measurements of saturated vapor densities. The saturated liquid density data in the critical region reported by Polikhronidi et al.[64] have been used for development of the crossover model for toluene. Vapor-pressure measurements for toluene in the critical region were performed by Mamedov and Akhundov,[65] Krase and Goodman,[74] Ambrose et al.,[75,76] and Griswold et al.[77]

Goodwin[73] developed a nonanalytical EOS for toluene for temperatures from the triple point (178.15 K) to 800 K, with pressures to 100 MPa using the *PVT* measurements by Straty et al.[59] and Akhundov and Abdullaev.[60,63] Franck et al.[62] developed a Tait-type EOS for toluene. A simplified EOS for toluene was developed by Mamedov et al.[65,78] Polt et al.[79] reported a Bender-type EOS with 20 parameters for toluene which were fit to the 685 *PVT* data by Akhundov and Abdullaev[60,63] and Marcos et al.[54] in the temperature range from 298 to 673 K and pressures up to 25 MPa. Recently, Lemmon and Jacobsen[80] developed a preliminary fundamental EOS for toluene which was obtained from a fit of the analytical multiparameter polynomial form to the available high-accuracy experimental *PVT*, C_P, and sound velocity,

toluene at infinite dilution as a function of state parameters were tested. The partial molar volumes at infinite dilution were obtained by extrapolation of the apparent molar volumes correlated as a function of the concentration. The uncertainties of the derived values of partial molar volumes are within 3−6 $cm^3 \cdot mol^{-1}$ at temperatures above 573 K.

The phase behavior of the water + toluene system belongs to type III mixtures. Figure 1 shows the $P-T$ phase diagram and the region of the $P-T$ plane for which values of the $PVTx$ data were measured for the water + toluene mixture. Figure 1 includes the available experimental data on the three-phase equilibrium curve, the critical curves, UCEP coordinates, vapor-pressure curves for pure components, and phase equilibria ($P-T$) curves for some selected compositions reported by Alwani[86] and Connolly[84] for the water + toluene mixture.

4. New *PVTx* Measurements

New measurements of the $PVTx$ properties for water + toluene mixtures have been performed with a constant-volume method which involves extracting samples from the piezometer under isothermal conditions. The method of measurements, experimental procedure, and construction of the piezometer have been discussed in detail elsewhere.[91−93] The main part of the apparatus for $PVTx$ measurements consisted of an air thermostat, a piezometer, lines for filling and extracting samples, temperature-control and temperature-measuring devices, and pressure-measuring instruments. A cylindrical piezometer horizontally mounted in the center of the air thermostat was used. The piezometer was made of heat- and corrosion-resistant high-strength alloy EI-437BU-VD. The thermostat has double walls and an inside volume of 65 dm^3. The heating elements were arranged between the walls. To minimize temperature gradients in the air thermostat, two electrically driven high-speed fans were used. The temperature inside the thermostat was maintained uniform within 5 mK with the aid of a guard heater located between the thermostat walls and the regulating heater that was mounted inside the thermostat. The temperature inside the thermostat and the fluid temperature was controlled automatically. The fluid temperature was detected by a platinum resistance thermometer (PRT-10) with a precision of 10 mK and was calibrated against the ITS-90 within an uncertainty of 1 mK. The resistance of the thermometer (PRT-10) at the water melting point is $R_0 = 9.9358 \pm 0.0005\ \Omega$. The temperature inside the thermostat was found during experimental runs to be the same as that of the sample water + toluene confined in the piezometer. The pressure exerted in the piezometer was transmitted to a liquid-octane system through a diaphragm-type null indicator that was mounted on the end of the piezometer and has a precision of ±2 kPa. The transferred liquid-octane pressure is transmitted to a dead-weight pressure gauge MP-600 with a resolution of 5 kPa. The diaphragm had a diameter of 40 mm and a thickness of 0.08 mm. A stirring ball was placed in the piezometer to agitate the mixtures.

The samples, water and toluene, were transferred separately from supply vessels into the piezometer using two hand-operated screw presses. The mass of a pure water mixture in the piezometer at given T and P was determined in a similar way. At first, the pure water was transferred into the piezometer. Then, the mass of the pure water m_w at a given temperature T and pressure P was obtained as $m_w = V_{TP}\rho_w$, where ρ_w is the pure water density, which was determined previously or calculated from IAPWS-95 formulation[83] and V_{TP} is the piezometer volume at given T and P which was determined by calibration. Next, the fill line of the piezometer was connected with the second-component injector, and the sample of pure hydrocarbon was injected into the piezometer until the desired pressure P was reached.

The mixture in the piezometer was heated in the thermostat until its temperature reached the prescribed value and the pressure reached a maximum value of about 45 MPa. After thermal equilibration, the $PVTx$ measurements along a selected isotherm were made, starting from a maximum pressure of about 45 MPa. Measurements were continued by extracting an appropriate amount of sample from the piezometer through a needle valve. The extracted samples were collected in a separate collector and weighed using a high-precision chemical balance with an uncertainty of 0.05 mg. Thus, several data points were taken along each isotherm until the system pressure became about 8 MPa.

The density of the sample at a given temperature T and pressure P is determined from the relations

$$\rho_i = M_i/V_{TP}, \quad M_i = m_{tot} - m_i\ (i = 1, 2, ..., N), \qquad m_{tot} = \sum_{i=1}^{N} m_i \quad (17)$$

where V_{TP} is the temperature- and pressure-dependent volume of the piezometer, M_i is the current mass of the water + hydrocarbon mixture in the piezometer after each extraction, m_i is the mass of the sample at each extraction from the piezometer during the runs, m_{tot} is the total mass or initial mass of the sample in the piezometer, and N is the number of extractions during the runs or number of experimental data points for each run. After the last extraction, the total mass, m_{tot}, of the water + toluene mixture in the piezometer was determined. The mass of toluene, m_{tot}, was determined from the difference between the total mass, m_{tot}, of the mixture extracted from the piezometer during the run and the known initial mass m_w of pure water in the piezometer, $m_{tol} = m_{tot} - m_w$. The density of the sample mixture for a given composition at a given temperature and pressure was determined using eq 17. The composition of the mixture was calculated from $x = 1 - m_w/m_{tot}$. The uncertainty of the mass m of the sample can be estimated from those of m_{tot} and m_i to be within 0.01%. The experimental uncertainty in the composition is estimated to be less than 0.001 mole fraction.

The inner volume of the piezometer was calculated by taking into consideration the corrections for elastic pressure deformation and thermal expansion. The volume of the piezometer was previously calibrated from the known density of a standard fluid (pure water) with well-known PVT values (IAPWS-95 formulation,[94,95] which has been fit to existing high-accuracy water data) at a temperature of $T_0 = 673.15$ K and a pressure of $P_0 = 40.32$ MPa. The authors claimed an uncertainty of the correlation[94] in this region to be $\delta\rho < 0.02\%$. The volume at these conditions was $V_{P_0T_0} = 32.68 \pm 0.01\ cm^3$.

Table 3. Experimental *PVTx* Data for Water + Tolune Mixtures at x = 2.87 Mol % of Toluene and Various Pressures (MPa)

density	temperature (K)										
(kg·m^{-3})	623.15	627.15	629.15	631.15	633.15	643.15	645.15	647.10	649.15	651.15	673.15
502.44	18.14	19.05	19.49	19.97	20.86	25.44	26.38	27.26	28.21	29.06	39.19
406.42	18.08	18.92	19.35	19.78	20.44	23.63	24.26	24.87	25.51	26.14	32.99
206.75	18.00	18.71	19.06	19.43	19.74	21.53	21.90	22.24	22.61	22.98	26.94
111.78	16.19	16.53	17.68	16.87	17.02	17.85	18.03	18.18	18.35	18.51	20.32
79.560	14.15	14.37	14.47	14.58	14.69	15.23	15.34	15.44	15.55	15.66	16.84
57.040	11.41	11.57	11.65	11.74	11.81	12.16	12.23	12.30	12.37	12.44	13.20

Table 4. Mixture Coefficients

parameter	water (k_{i0})	toluene (k_{i1})	$k_i^{(1)}$	$k_i^{(2)}$
		Critical Amplitudes		
k	1.413 80	1.024 58	−4.1776	4.1893
d_1	$-7.133\ 19 \times 10^{-1}$	$8.461\ 47 \times 10^{-1}$	0.5862	1.9908×10
a	$2.253\ 83 \times 10$	$2.331\ 77 \times 10$	-1.4994×10	-6.6113×10
c_1	−6.837 12	$-1.844\ 37 \times 10$	-6.7479×10	1.9677×10^2
c_2	$1.332\ 15 \times 10$	$2.599\ 52 \times 10$	0	0
c_3	$-1.162\ 19 \times 10$	$1.692\ 44 \times 10$	−2.2191	-2.4752×10^2
c_4	7.835 68	$-2.124\ 23 \times 10$	2.2675×10	2.5603×10^2
		Crossover Parameter		
g	$1.801\ 52 \times 10^{-5}$	1.296 14	−4.0512	3.0924×10^2
		Background Coefficients		
A_1	−7.810 74	−7.260 66	6.6065	8.2305
A_2	$1.811\ 22 \times 10$	$2.091\ 85 \times 10$	-5.2671×10	2.4531×10
A_3	2.720 22	$1.013\ 13 \times 10$	0	0
$\Delta m_1 = m_{11} - m_{10}$	0	0	−1.3480	0
m_1	$-2.073\ 84 \times 10$	0	2.5494	−2.9518
m_2	$-1.141\ 68 \times 10$	$-4.779\ 20 \times 10$	3.4528×10	0
m_3	6.237 49	$-3.964\ 90 \times 10^{-1}$	-1.0180×10	0
m_4	−6.418 86	$-5.090\ 24 \times 10^{-1}$	0	0
		Molecular Weight		
M_W	18.0152	92.134	0	0

Variations of the volume depending on temperature T and pressure P were calculated from the equation

$$V_{TP} = V_{T_0P_0}[1 + 3\alpha_T(T - T_0) + \beta_P(P - P_0)] \quad (18)$$

where $\alpha_T = 1.3 \times 10^{-5}$ K^{-1} is the thermal expansion coefficient of the alloy (EI-437BU-VD), which is virtually temperature-independent in the temperature range from 500 to 700 K, and $\beta_P = 4.12 \times 10^{-5}$ MPa^{-1} is the pressure expansion coefficient of the piezometer. The values of α_T and β_P for this piezometer were determined experimentally using *PVT* data for pure water calculated from the IAPWS-95 formulation[83,84] with uncertainties of 8−10%. The maximum uncertainty in the volume of the piezometer δV_{TP} at a given temperature T and pressure P is related to the measured uncertainties of $V_{T_0P_0}$, α_T, and β_P, which were $\delta V_{T_0P_0} \approx 0.03\%$, 0.0012%, and 0.0005%, respectively. Therefore, the values of δV_{TP} in the worst case are about 0.032%. The present experimental apparatus had no "dead volumes". Taking into account the uncertainties of temperature, pressure, and concentration measurements, the total experimental uncertainty in density was estimated to be within 0.05−0.2%, depending on the temperature T and pressure P.

The experimental results for the *PVTx* relationship for the water + toluene mixture at a concentration of $x = 0.0287$ mole fraction of toluene along 11 near-critical and supercritical isotherms are given in Table 3. Measurements have been made at T = 623, 627, 629, 631, 633, 643, 645, 647, 649, 651, and 673 K and pressures up to 39 MPa at a composition of 0.0287 mole fraction of toluene. The shaded area in Figure 1 marks the temperature−pressure region where the new *PVT* data for the water + toluene mixture at $x = 0.0287$ have been obtained.

5. Crossover Free-Energy for Water + Toluene Mixtures

To use the parametric crossover model defined by eqs 1−6, together with eqs 14 and 15, one needs to know the system-dependent coefficients k, d_1, a, c_i, g, A_i, and m_i for pure components ($\tilde{x} = 0$ and $\tilde{x} = 1$) and the critical locus. For pure water ($\tilde{x} = 0$), we adopted the critical parameters T_{c0}, ρ_{c0}, and P_{c0} and coefficients k_0, d_{10}, a_0, c_{i0}, g_0, A_{i0}, and m_{i0} reported earlier by Kiselev and Friend.[96] For pure toluene ($\tilde{x} = 1$), we adopted the critical parameters T_{c1}, ρ_{c1}, and P_{c1}, as reported by Polikhronidi et al.,[64] while the coefficients k_1, d_{11}, a_1, c_{i1}, g_1, A_{i1}, and m_{i1} were found from a fit of eqs 1−6 to the *PVT* data sets by Akhundov and Abdullaev[60,63] and Straty et al.[59] together with isobaric heat capacity data of Akhundov et al.[65,97] in the range of temperatures and densities bounded by

$$\tau + 1.2\Delta\rho^2 \le 0.5, \quad T \ge 0.98T_c \quad (19)$$

This range of validity of the parametric crossover model is the same as that reported earlier by Kiselev and Friend[96] for pure water. The values of all system-dependent coefficients for pure components and water + toluene mixtures are listed in Table 4.

Once the pure-fluid EOSs for the components of a binary mixture are known, only the critical locus of the binary mixture is needed in order to predict the thermodynamic properties and the phase behavior of the mixture. Unfortunately, except for a few P_c−T_c points

Table 5. Critical Parameters

			Pure Water		
P_{c0}, MPa	22.064	T_{c0}, K	647.096	ρ_{c0}, mol·L^{-1}	17.874
			Mixture Coefficients		
P_1, MPa·K^{-1}	1.0666×10^{-1}	T_1, K	-8.1025×10^{2}	ρ_1, mol·L^{-1}	-1.7498×10
P_2, MPa·K^{-2}	-2.3062×10^{-4}	T_2, K	1.6892×10^{4}		
P_7, MPa·K^{-7}	3.94635×10^{-12}	T_3, K	-1.1061×10^{5}		
P_8, MPa·K^{-8}	7.50993×10^{-14}				
			Pure Toluene		
P_{c1}, MPa	4.2337	T_{c1}, K	593.884	ρ_{c1}, mol·L^{-1}	3.1950

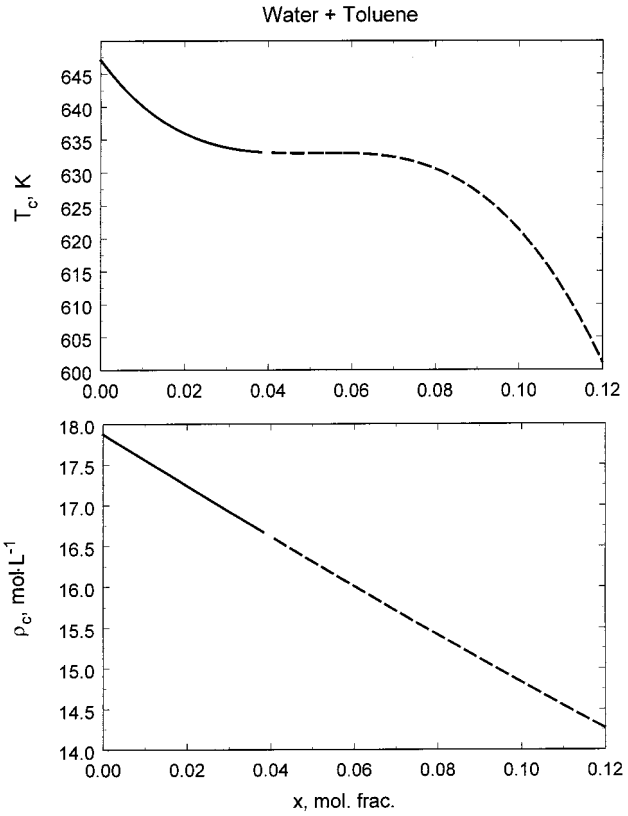

Figure 2. Critical temperature, T_c (top), and critical density, ρ_c (bottom), for water + toluene mixtures calculated with the CREOS as a function of the mole fraction of toluene, x.

obtained by Alwani and Schneider,[87] we do not know of any other critical locus data for dilute water + toluene mixtures. Therefore, in the present work we have solved an inverse task: we found the critical locus for dilute water + toluene mixtures from the CREOS, using in eqs 14 and 15 the values of the mixture coefficients $k_i^{(j)}$ (j = 1 and 2) which we found earlier for type I mixtures.[31] We did this in two steps. First, we found the coefficients P_i (i = 1, 2, 7, and 8) from a fit of eq 11 to the P_c-T_c data of Alwani and Schneider[87] in the temperature range 585 K < $T_c(\tilde{x}) \leq T_{c0}$. Second, we found the coefficients T_1, T_2, T_3, and ρ_1 in eqs 9 and 10 from a fit of the crossover model (with the fixed values of the coefficients P_1, P_2, P_7, and P_8) to our new *PVT* data for water + toluene mixtures at x = 0.0287 and to the one-phase *PVTx* data obtained by Degrange[38] at x = 0.0012−0.0366 mole fraction of toluene. The values of the coefficients P_i, T_i, and ρ_1 for dilute water + toluene mixtures are listed in Table 5, and the critical locus calculated with these coefficients is shown in Figure 2. The dashed curves in Figure 2 correspond to the extrapolations of the critical lines to higher concentrations where no experimental *PVTx* data were used for their determination. As one can see, in the entire region $x \leq 0.12$ the critical density $\rho_c(x)$ is an almost linear function of x, while the critical temperature $T_c(x)$ at $x > 0.03$ is a nonmonotonic function of x that, at higher concentrations, somewhere at $x > 0.12$, should pass through the minimum, as shown in Figure 1.

Table 6. Deviation Statistics for Thermodynamics Properties of Pure Toluene

	PVT		C_P,	W,
	Akhundov and Abdullaev[60,63]	Straty et al.[59]	Akhundov et al.[97]	Pankevich and Zotov[100]
AAD	0.31	0.45	1.07	2.64
BIAS	0.13	−0.37	−0.01	−2.29
SDV	0.38	0.54	1.41	2.12
RMS	0.03	0.05	0.15	0.47
MAXDEV	−1.39	−2.15	6.13	−5.63
N	169	108	84	20

6. Comparison with Experimental Data

6.1. Pure Components. The accuracy of the crossover EOS for pure water in the near-critical and supercritical regions was examined in detail in our previous papers (see refs 96 and 98); therefore, we will not discuss it here. The accuracy and reliability of the crossover model for pure toluene in the near-critical and supercritical regions were examined statistically in terms of the absolute average deviation (AAD), the bias (BIAS) and standard deviation (SDV), the root-mean-square deviation (RMS), and the maximum percentage deviation (MAXDEV) with respect to each data set as summarized in Table 6. The relative percentage deviations between measured and calculated values of pressures, isobaric heat capacities, and sound velocity are presented in Figures 3−5. Most *PVT* data reported by Straty et al.[59] in the density range from 100 to 420 kg·m^{-3} show deviations within ±1.0% in pressure (only one point shows a deviation of more than 2%, and 11 data points show deviations of more than 1%), while the data by Akhundov and Abdulaaev[60,63] in the same density and temperature ranges show deviations within ±0.5% in pressure. Almost all of the *PVT* data by Akhundov and Abdulaaev[60,63] deviate from the values calculated by CREOS within ±1.0%. Only two data points show deviations of more than 1%. The agreement between measurements by Akhundov et al.[97] and calculated values from CREOS for the isobaric heat capacity is excellent (AAD = 1%). The C_P data of toluene reported by Nefedov and Filippov[99] along the isotherms 600 and 620 K deviate from calculated values by 1.2%. Figure 5 shows the representation of the sound velocity data reported by Pankevich and Zotov.[100] For these data the AAD is about 2.64%. Most data at high densities (ρ > 435 kg·m^{-3}) show systematically negative deviations.

For the VLE calculations in mixtures, it is important to be able to extrapolate the CREOS to low temperatures and high densities, beyond the boundary given by

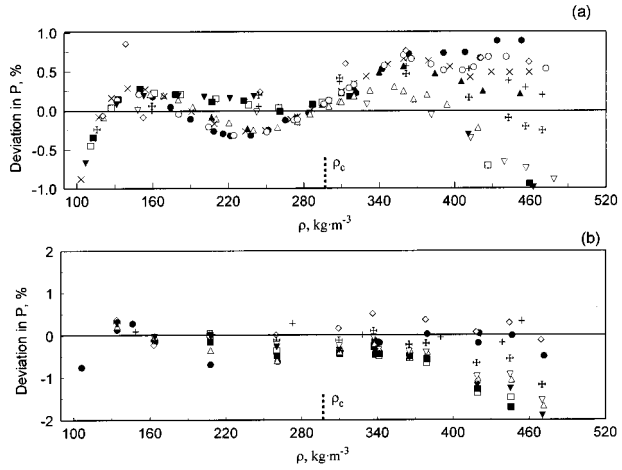

Figure 3. Percentage deviations, $100(P^{exp} - P^{cal})/P^{exp}$, between experimental results for the pressure of pure toluene by Akhundov and Abdullaev[60,63] (a) and by Straty et al.[59] (b) and values calculated with the CREOS (present work): ●, 593.15 K; ○, 595.15 K; ×, 596.15 K; ▲, 598.15 K; △, 603.15 K; ■, 613.15 K; □, 623.15 K; ▼, 633.15; ▽, 643.15 K; □, 653.15; +, 663.15 K; ◊, 673.15 K.

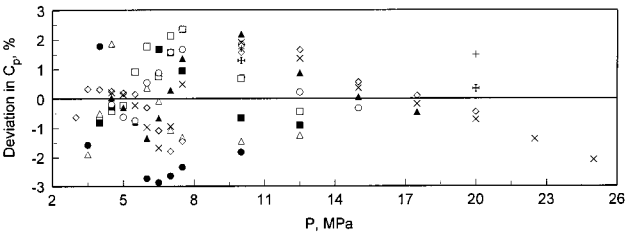

Figure 4. Percentage deviations, $100(C_P^{exp} - C_P^{cal})/C_P^{exp}$, between experimental results for the isobaric heat capacity of pure toluene by Akhundov et al.[65,97] (●, 603.15 K; ○, 643.15 K; ×, 663.15 K; ▲, 653.15 K; △, 613.15 K; ■, 623.15 K; □, 633.15 K; ◊, 673.15 K) and by Nefedov and Filippov[99] (□, 620.15 K; +, 600.15 K) and values calculated with the CREOS (present work).

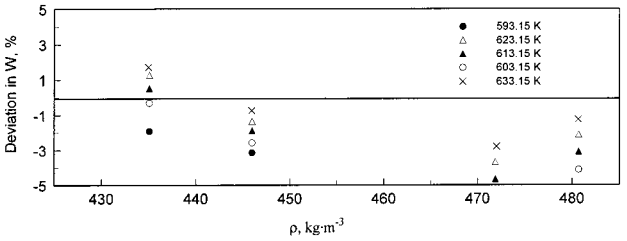

Figure 5. Percentage deviations, $100(W^{exp} - W^{cal})/W^{exp}$, between experimental results for the sound velocity of pure toluene by Pankevich and Zotov[100] and values calculated with the CREOS (present work): ●, 593.15 K; ○, 603.15 K; ▲, 613.15 K; △, 623.15 K; ×, 633.15 K.

eq 19. The comparisons of the vapor pressure, saturated densities, and sound velocities along the coexistence curve down to $T = 550$ K (or $0.93 < T/T_c \leq 1$) are given in Figures 6−8. These figures contain also the data sets reported by other authors that were not used in the optimization procedure. The densities of the saturated liquid and saturated vapor measured by Polikhronidi et al. in the critical region are reproduced by CREOS to within 1.6% and 1%, respectively, while the saturated liquid density data by Mamedov and Akhundov[65] are reproduced within 1.6%. The comparison of the vapor-pressure data by Mamedov and Akhundov[65] with the crossover model shows that the deviations are within 0.05% in the temperature range from 563 K to the critical point. Good agreement is found between the data of Ambrose[76] and the CREOS at low temperatures

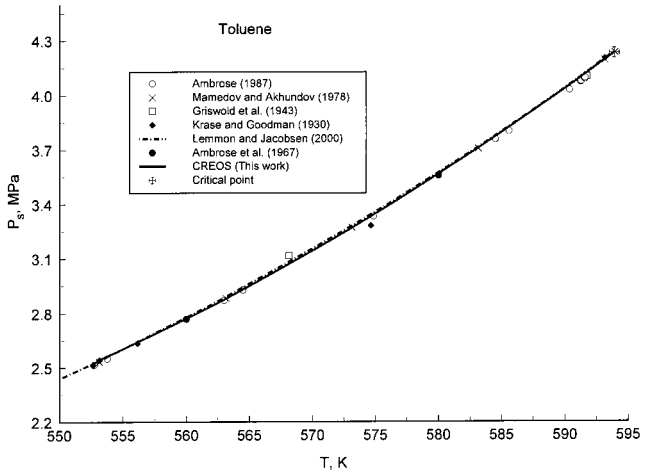

Figure 6. Vapor-pressure curve of pure toluene near the critical point by various authors together with values calculated with the multiparametric EOS of Lemmon and Jacobsen[80] (dash-dotted line) and with the CREOS (solid line).

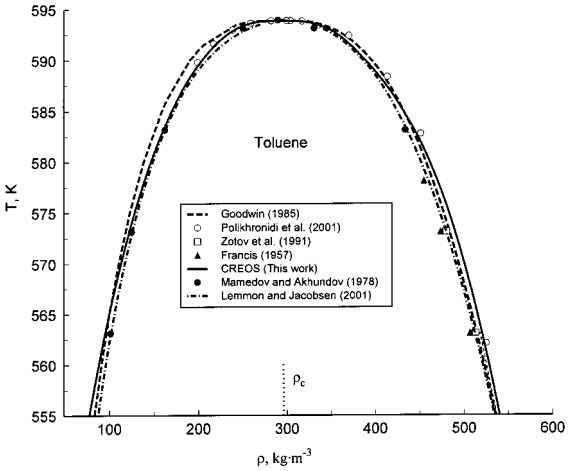

Figure 7. Coexistence curve of pure toluene near the critical point by Polikhronidi et al.,[64] by Zotov et al.,[66] by Francis,[72] and by Mamedov and Akhundov[65] together with the values calculated from Goodwin[73] (dashed line), with the multiparametric EOS of Lemmon and Jacobsen[80] (dash-dotted line) and with the CREOS (solid line).

($T < 585$ K), while in the immediate vicinity of the critical point, the deviations are systematically negative (0.1−0.2%). Reasonable agreement (about 1.7%) is observed for sound velocity between the data reported by Zotov[101] and the model in the temperature range above 570 K.

Comparisons of essential thermodynamic properties (*PVT*, isobaric heat capacity, and sound velocity) in the extended density region along separate supercritical isotherms for pure toluene with values calculated with the crossover model are shown Figures 9−12. The other model with which we compared is a preliminary fundamental EOS for toluene developed by Lemmon and Jacobsen.[80] Except in the nearest vicinity of the critical point where the analytical EOS of Lemmon and Jacobsen[80] fails to reproduce the critical depression of the sound velocity (see Figure 8), this multiparameteric EOS has excellent reproducibility in the supercritical region. The *PVT* data by Akhundov and Abdullaev[60,63] and Straty et al.[59] are almost equally well represented by the present crossover model and the Lemmon and Jacobsen[80] model. As one can see from Figures 10 and 11, small discrepancies between the CREOS and mul-

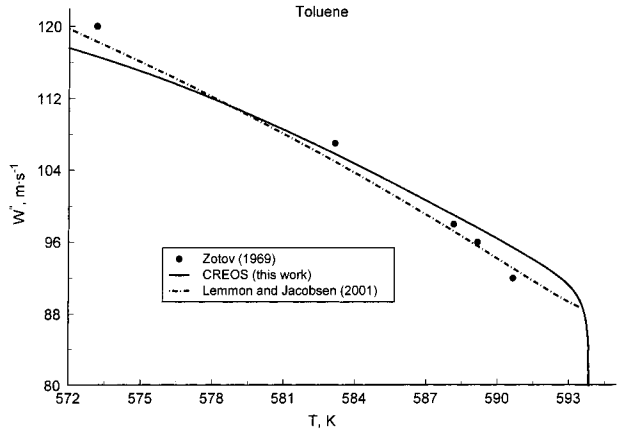

Figure 8. Vapor sound velocity, W, of pure toluene along the saturation curve as a function of temperature, T. The symbols represent experimental data by Zotov,[101] and the lines correspond to the values calculated with the multiparametric EOS of Lemmon and Jacobsen[80] (dash-dotted line) and with the CREOS (solid line).

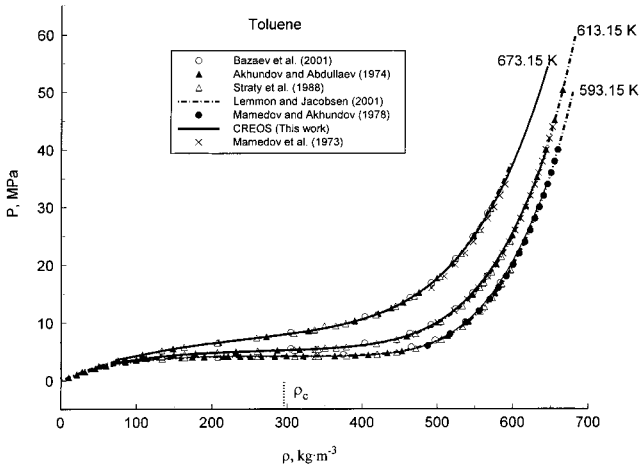

Figure 9. Pressure, P, of pure toluene along the separate isotherms as a function of density, ρ. The symbols represent experimental data by Bazaev,[131] by Akhundov and Abdulaev,[60] by Straty et al.,[59] and by Mamedov and Akhundov,[65] and the lines correspond to the values calculated with the multiparametric EOS of Lemmon and Jacobsen[80] (dash-dotted line) and with the CREOS (solid line).

tiparametric EOS of Lemmon and Jacobsen[80] are observed for the isobaric heat capacity, C_P at high pressures, $P \geq 150$ MPa, where the densities are greater than $2\rho_c$ (see Figure 9). However, even in this region, the maximum deviations between values calculated with the CREOS and experimental C_P data do not exceed 2%.

6.2. Aqueous Toluene Solutions. The deviation plots for the new $PVTx$ data for water + toluene mixtures and data set by Degrange[38] are depicted in Figures 13 and 14. The deviation statistics are given in Table 7. For both data sets, most data show deviations within ±1.0%. Figure 15 shows direct comparisons between measured and calculated values of pressure for water + toluene mixtures along various near-critical and supercritical isotherms. Figure 16 shows the compressibility factor $Z = PV/RT$ for the water + toluene mixture at $x = 0.0287$ mole fraction of toluene as a function of pressure along some near-critical and supercritical isotherms. Figure 16 also contains results for pure water calculated with CREOS by Kiselev and Friend.[96] In all cases, good agreement between experimental data and calculated values is observed.

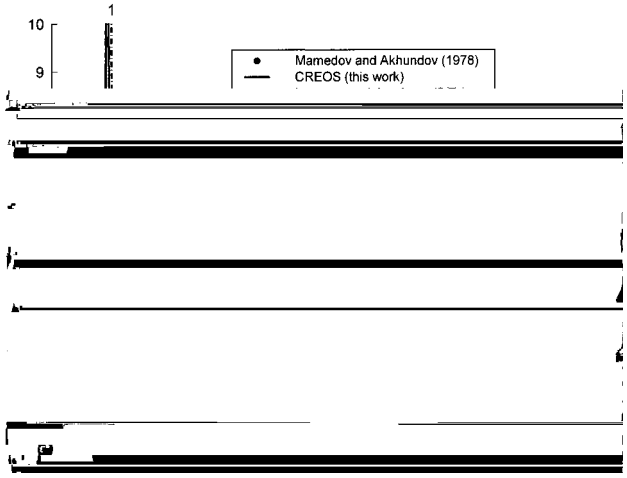

Figure 10. Isobaric heat capacity, C_P, of pure toluene along the separate isotherms as a function of pressure, P. The symbols represent experimental data by Mamedov and Akhundov,[65] and the lines correspond to the values calculated with the multiparametric EOS of Lemmon and Jacobsen[80] (dash-dotted line) and with the CREOS (solid line).

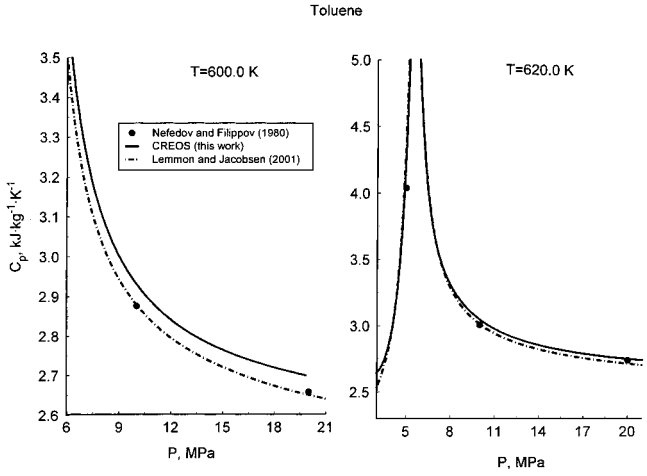

Figure 11. Isobaric heat capacity, C_P, of pure toluene measured by Nefedov and Filippov[99] (symbols) along two isotherms as a function of pressure, P, together with values calculated with the multiparametric EOS of Lemmon and Jacobsen[80] (dash-dotted lines) and with the CREOS (solid lines).

From a practical point of view, it is interesting to know how far in terms of temperature and composition the CREOS can be extrapolated from the critical point of pure water to give a reasonable representation of the thermodynamic properties and phase behavior of water + toluene mixtures. Theoretically, if the critical locus is known, the only restriction on the CREOS is given by eq 19. In this case, the extrapolation range in temperatures and densities should be approximately the same as those for the pure components, as discussed above. For water + toluene mixtures the critical locus was determined from a fit of the crossover model to the one-phase $PVTx$ data at $x < 0.04$, and extrapolation of the CREOS to higher concentrations provides a good test for the thermodynamic consistency of the model. Figure 17 shows comparisons between experimental VLE data obtained by Alwani[86] and Alwani and Schneider[87] at two compositions, $c = 30$ and 40 wt % of toluene ($x = 0.07732$ and 0.11532 mole fraction of toluene, respectively), with the values calculated with the crossover model. As one can see, with temperatures $T \geq 590$ K at $c = 30$ wt % and $T \geq 580$ K at $c = 40$ wt

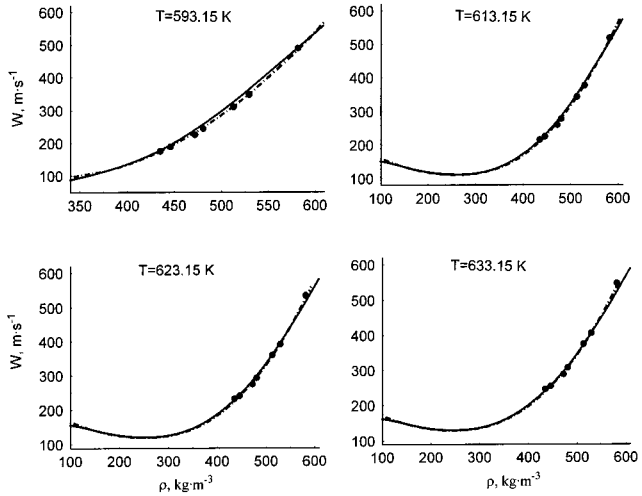

Figure 12. Sound velocity, W, of pure toluene as a function of density, ρ, along near critical and supercritical isotherms. The symbols represent experimental data by Zotov,[101] and the lines correspond to the values calculated with the multiparametric EOS of Lemmon and Jacobsen[80] (dash-dotted lines) and with the CREOS (solid lines).

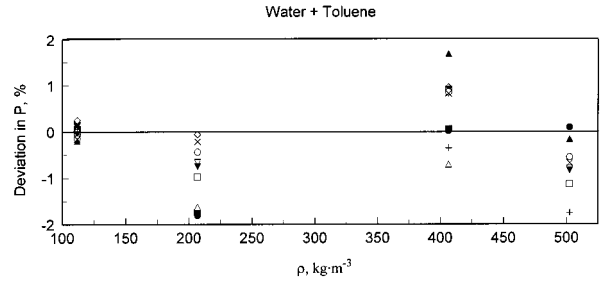

Figure 13. Percentage deviations, $100(P^{exp} - P^{cal})/P^{exp}$, between present experimental results for the pressure of water +toluene mixtures at x = 0.0287 mole fraction of toluene and values calculated with the CREOS: ◊, 623.15 K; ●, 627.15 K; +, 629.15 K; △, 631.15 K; ■, 633.15 K; □, 643.15 K; ▼, 645.15 K; ▽, 647.15 K; ○, 649.15 K; ×, 651.15 K; ▲, 673.15 K.

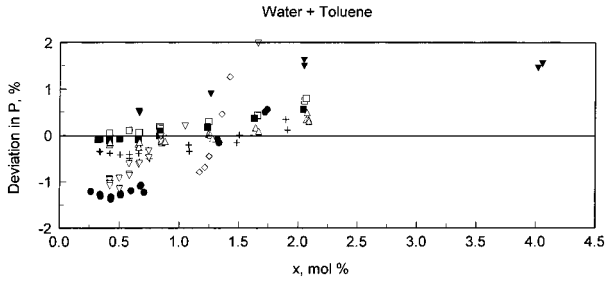

Figure 14. Percentage deviations, $100(P^{exp} - P^{cal})/P^{exp}$, between experimental results for the pressure of water + toluene mixtures by Degrange[38]and values calculated with the CREOS: ◊, 643.15 K and 28.00 MPa; ●, 658.52 and 28.15 MPa; +, 664.95 K and 28.15 MPa; △, 667.93 K and 28.10 MPa; ■, 670.20 and 28.15 MPa; □, 645.04 K and 28.15 MPa; ▼, 685.17 and 28.10 MPa; ▽, 664.92 K and 33.10 MPa.

%, the crossover model yields an adequate representation of the VLE data by Alwani.[86] Thus, similar to pure toluene, the CREOS for water + toluene mixtures can be extrapolated into the low-temperature region $0.93 < T/T_c(x) \leq 1$. This justifies the extrapolation of the critical locus for water + toluene mixtures at concentrations up to $x = 0.12$ mole fraction of toluene shown in Figure 2 by dashed lines.

6.3. Infinitely Dilute Solutions. The thermodynamic behavior of near-critical dilute solutions is extremely important for understanding the molecular interactions and the microscopic structure of the solutions. In the limit of infinite dilution, many partial molar properties of the solute ($\bar{V}_2^\infty$, $\bar{H}_2^\infty$, $\bar{C}_{P2}^\infty$) diverge strongly at the solvent's critical point.[8,102−108] In general, the thermodynamic behavior of infinitely dilute mixtures near the solvent's critical point can be completely characterized by the so-called Krichevskii parameter (which is equal to the derivative $(\partial P/\partial x)_{T_c V_c}^\infty$ calculated

Table 7. Deviation Statistics for *PVTx* Properties of the Water + Toluene Mixture

	PVTx	
	Degrange[38]	this work
AAD	0.56	0.91
BIAS	−0.16	−0.43
SDV	0.76	1.05
RMS	0.07	0.19
MAXDEV	−2.51	2.93
N	115	32

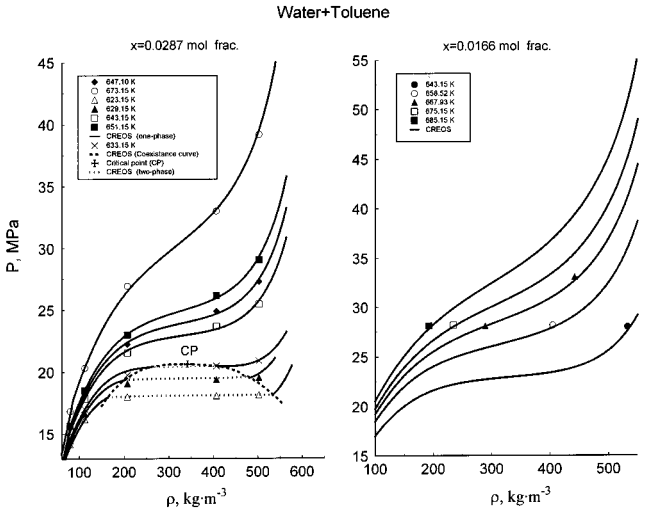

Figure 15. Pressure, P, of the water + toluene mixture as a function of density, ρ, along the near-critical and supercritical isotherms at $x = 0.0287$ and 0.0166 mole fractions of toluene. The symbols represent our experimental data of this work (left) and those by Degrange[38] (right), and the lines correspond to the values calculated with the CREOS into the one (solid lines) and two phases (dotted and dashed lines).

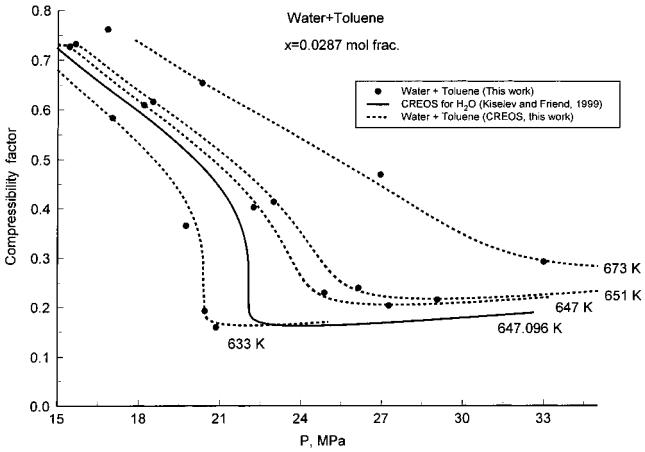

Figure 16. Compressibility factor, $Z = PV/RT$, for the water + toluene mixture as a function of pressure, P, along the near-critical and supercritical isotherms (symbols) together with the values calculated with the CREOS at $x = 0.0166$ mole fraction of toluene (dashed lines) and pure water (solid line).

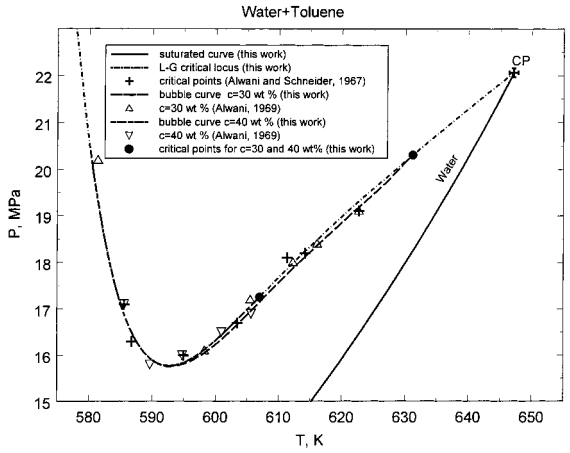

Figure 17. Comparison of the experimental values of the critical pressure (pluses) and the VLE data (triangles) for water + toluene mixtures reported by Alwani[86] at $c = 30$ and 40 wt % toluene ($x =$ 0.07732 and 0.11532 mole fractions of toluene, respectively) with the values calculated with the CREOS (filled circles and lines).

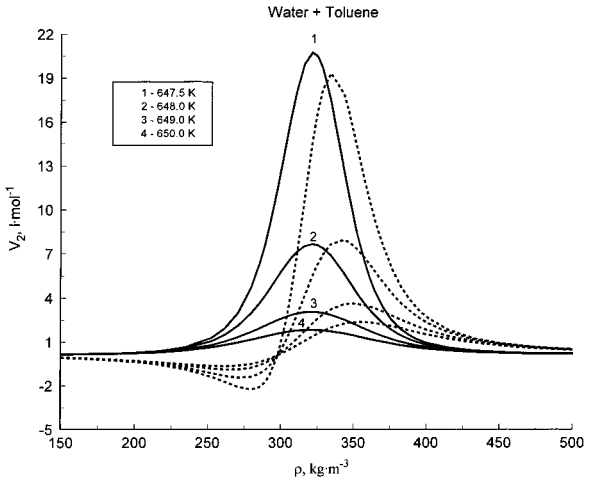

Figure 18. Comparison of the partial molar volume, $\bar{V}_2^{\infty}$, in the water + toluene mixture calculated with the CREOS (solid lines) and with the semiempirical equation by Majer et al.[90] (dashed lines) in the supercritical region.

at the critical point of pure solvent[102,103,109−115]). Using the concept of the Krichevskii parameter, Levelt Sengers[116] proposed a description of the thermodynamic behavior of dilute near-critical solutions based on the derivative $(\partial P/\partial x)_{VT}^{\infty}$, and Japas et al.[117] denoted $(\partial P/\partial x)_{VT}^{\infty}$ as the Krichevskii function. The Krichevskii function is related to the direct correlation functions[12,15,118−122] and takes into account the effects of the intermolecular interactions between solvent and solute molecules that determine the thermodynamic properties of dilute solutions. The value of the Krichevskii function at the critical point of pure solvent is the exact Krichevskii parameter.[123,124]

In this work, we used the CREOS to calculate the Krichevskii parameter in water + toluene mixtures

$$\left(\frac{\partial P}{\partial x}\right)_{T_c V_c}^{\infty} = 136.3 \text{ MPa·mol}^{-1} \tag{20}$$

The value of this parameter was estimated also from the initial slopes of the critical lines for water + toluene mixtures and the values of the vapor-pressure slope of pure water at the critical point. The initial slopes of the critical lines are related to the Krichevskii parameter as follows:[123,125−127]

$$\left(\frac{\partial P}{\partial x}\right)_{T_c V_c}^{C} = \left(\frac{\partial P_c}{\partial x}\right)_{CRL}^{C} - \left(\frac{dP_S}{dT}\right)_{CXC}^{C}\left(\frac{\partial T_c}{\partial x}\right)_{CRL}^{C} \tag{21}$$

or, equivalently,

$$\left(\frac{\partial P}{\partial x}\right)_{T_c V_c}^{C} = \left[\left(\frac{dP_c}{dT_c}\right)_{CRL}^{C} - \left(\frac{dP_S}{dT}\right)_{CXC}^{C}\right]\left(\frac{dT_c}{dx}\right)_{CRL}^{C} \tag{22}$$

where $(\partial P_c/\partial x)_{CRL}$ and $(\partial T_c/\partial x)_{CRL}^{C}$ are the initial slopes of the $P_c(x)$ and $T_c(x)$ critical lines and $(dP_S/dT)_{CXC}^{C}$ is the slope of the solvent's vapor-pressure curve evaluated at the critical point of the solvent (always positive). Qualitatively and quantitatively the behavior of near-critical dilute solutions depends strongly on the signs and the magnitudes of the initial slopes of the $T_c(x)$, $P_c(x)$, and vapor-pressure curves in the critical point of pure solvent. Therefore, the Krichevskii parameter is a good test for the thermodynamic consistency of the model. We calculated the Krichevskii parameter for the dilute water + toluene mixtures with eqs 21 and 22, where the derivative $(dP_S/dT)_{CXC}^{C}$ was calculated with the vapor-pressure equation given by Levelt Sengers[128] and the slopes of the critical lines $T_c(x)$ and $P_c(x)$ were calculated with the crossover model. The results are $(dP_S/dT)_{CXC}^{C} = 0.2682$ MPa·K^{-1}, $(\partial P_c/\partial x)_{CRL} = -91.033$ MPa·mol^{-1}, $(\partial T_c/\partial x)_{CRL}^{C} = -853.494$ K·mol^{-1}, and $(dP_c/dT_c)_{CRL}^{C} = 0.1067$ MPa·K^{-1} and the Krichevskii parameter is $(\partial P/\partial x)_{T_c V_c}^{\infty} = 137.7$ MPa·mol^{-1}, which practically coincides with our previous result given in eq 20.

The value of the Krichevskii parameter for the water + toluene mixture was also estimated by Plyasunov and Shock[129] from the empirical relation

$$\left(\frac{\partial P}{\partial x}\right)_{T_c V_c}^{\infty} = 88.7 + 4.11\Delta G° \tag{23}$$

(where ΔG^0 is a difference between the Gibbs energy of a solute at 298.15 K and 0.1 MPa and the energy of sublimation) and from the values of the partial molar volume $\bar{V}_2^{\infty}$ derived by Degrange[38] from the *PVTx* measurements. The derived value from the partial molar volume of the Krichevskii parameter is 105 ± 10 MPa·mol^{-1}, and the estimate value calculated with eq 23 gives $(\partial P/\partial x)_{T_c V_c}^{\infty} = 107$ MPa·mol^{-1}. The agreement between our results and the values reported by Plyasunov and Shock[129] is reasonably good.

There are no experimental data for the partial molar volume $\bar{V}_2^{\infty}$ in dilute aqueous toluene solutions. Therefore, in Figure 18 we show the comparison between the values of the partial molar volume in the infinitely dilute aqueous toluene solutions calculated with the crossover model using the relation[13]

$$\bar{V}_2^{\infty} = V_{H_2O}\left[1 + K_T^{H_2O}\left(\frac{\partial P}{\partial x}\right)_{VT}^{\infty}\right] \tag{24}$$

and with the semiempirical model of Majer et al.[90]

$$\bar{V}_2^{\infty} = V_{H_2O} + RTK_T^{H_2O}\rho_w[a_1 + a_2[\exp(v\rho_{H_2O}) - 1]] \tag{25}$$

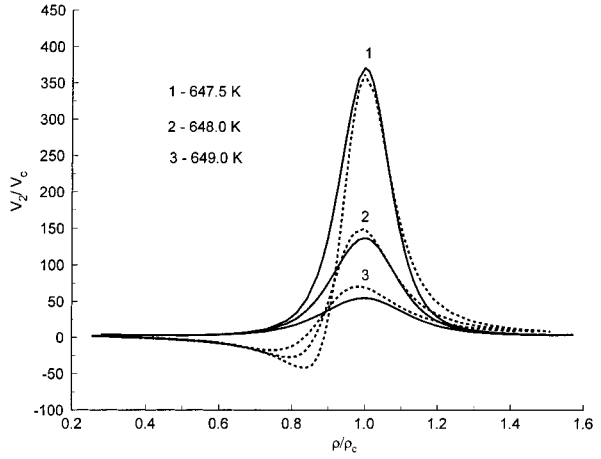

Figure 19. Reduced partial molar volume $\bar{V}_2^{\infty}/V_c^{H_2O}$ as a function of reduced density $\rho/\rho_c^{H_2O}$ along the near-critical isotherm in the water + toluene mixture. Solid lines are from CREOS (present work), and dashed lines are from the semiempirical equation by Majer et al.[90]

In eqs 24 and 25, V_{H_2O} is the molar volume of pure water, $K_T^{H_2O}$ is the compressibility of pure water, ρ_w is the density of pure water, the specific volume $v = 5$ cm^3·g^{-1}, and a_1, a_2, and a_3 are the system-dependent parameters which were found from the experimental values of the partial molar volume of toluene in an infinitely dilute water + toluene mixture.[90] Equation 25 is valid in the temperature range from 298 to 623 K. However, to compare it with our crossover model, we extrapolated this equation to high temperatures. The results are shown in Figure 18. Far from the critical region (at densities lower than 200 kg·m^{-3} and higher than 400 kg·m^{-3}), the agreement between the two estimates is good. However, in the critical region some systematic deviations between these two models are observed. The partial molar volume calculated with eq 25 exhibits a maximum at a density of about 335 kg·m^{-3}, which is slightly higher than the critical density of pure water ($\rho_c^{H_2O} = 322.0$ kg·m^{-3}) adopted in our crossover model. Therefore, the large systematic deviations between our results and the values calculated with eq 25 in the critical region can be explained by the difference in the critical density in our model and in the empirical EOS used by Majer et al.[90] Figure 19 shows the partial molar volumes for dilute water + toluene solutions in the reduced coordinates, $\bar{V}_2^{\infty}/V_c^{H_2O}$ versus $\rho/\rho_c^{H_2O}$, where $V_c^{H_2O}$ and $\rho_c^{H_2O}$ for each model were used. As one can see, except in the low-density region where the partial molar volumes calculated with the crossover model and with the semiempirical model of Majer et al.[90] exhibit opposite signs for $\bar{V}_2^{\infty} - \rho$ slopes, the agreement between these two methods is fairly good.

7. Discussion

In the present work, we reported new *PVTx* measurements and developed the crossover Helmholtz free-energy model for the water + toluene binary mixture in a wide vicinity around the critical point of pure water. For this purpose, we used the parametric crossover model (CREOS97) developed earlier for type I binary mixtures.[31,42] Unlike the previous studies, where the critical locus was used as an input in the crossover model,[31,32,42,47] here we found the critical locus from a fit of the CREOS to the one-phase *PVTx* data at $x <$ 0.04 mole fraction of toluene. By direct comparison with existing experimental data, we show that the CREOS not only yields a good representation of the thermodynamic surface for dilute aqueous solutions but also can be extrapolated at higher concentrations, up to $x = 0.12$ mole fraction of toluene. This allows us to make an important prediction concerning the crossover behavior of the isochoric heat capacity, $C_{V,x}$, in water + toluene mixtures. According to theoretical considerations,[20,24,25,130] an asymptotic behavior of $C_{V,x}$ along the critical isochore $\rho = \rho_c(x)$ in a binary mixture at fixed composition x is determined by the characteristic temperature

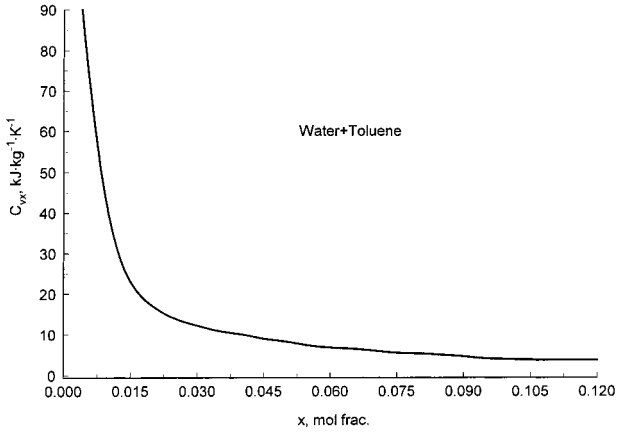

Figure 20. Isochoric heat capacity, $C_{V,x}$, along the critical line of dilute water + toluene mixtures calculated with the CREOS as a function of concentration, x.

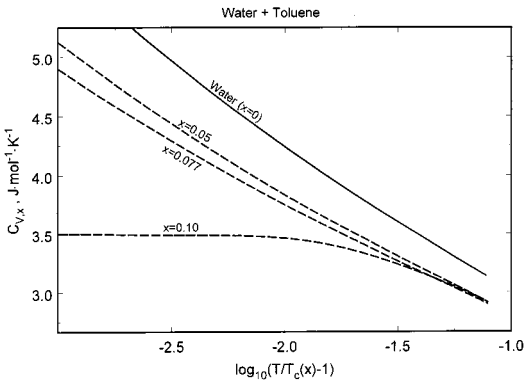

Figure 21. Isochoric heat capacity, $C_{V,x}$, in water + toluene mixtures along the critical isochore $\rho = \rho_c(x)$ at various compositions calculated with the CREOS as a function of the dimensionless temperature $\tau(x) = T/T_c(x) - 1$.

$$\tau_\alpha(x) \cong \left[A_0 x(1-x)\left(\frac{1}{T_c(x)}\frac{dT_c}{dx}\right)^2\right]^{1/\alpha} \qquad (26)$$

In the temperature range $\tau_\alpha(x) \ll \tau(x) \ll 1$, the isochoric heat capacity at constant x behaves according to the scaling law behavior of C_V in one-component fluids:

$$C_{V,x}/R \simeq A_0\tau(x)^{-\alpha} + \text{Const} \qquad (27)$$

However, asymptotically close to the critical point, such as

$$\tau(x) \ll \tau_\alpha(x) \qquad (28)$$

the renormalization of the critical exponent $\alpha \rightarrow -\alpha/(1-\alpha)$ takes place, and $C_{V,x}$ on the critical isochore exhibits mixturelike behavior

$$C_{V,x} \simeq \text{Const} - A_0\tau(x)^{\alpha/(1-\alpha)} \quad (29)$$

Figure 20 shows the concentration dependence of the isochoric heat capacity along the critical curve. The temperature dependence of $C_{V,x}$ along the critical isochore in water + toluene mixtures is shown in Figure 21. One can see that at $x \leq 0.08$ the parameter τ_α is small ($\tau_\alpha \ll 10^{-3}$) and in the entire experimentally available region ($10^{-4} < \tau < 1$) $C_{V,x}$ in water + toluene mixtures behaves like C_V in pure water (see eq 27). However, at $x = 0.1$ the parameter $\tau_\alpha \simeq 10^{-1}$ is not small, and at $\tau \ll 10^{-1}$ the renormalization given by eq 29 is observed. Thus, $C_{V,x}$ in a water + toluene mixture at $x = 0.1$ mole fraction of toluene exhibits mixturelike behavior (eq 29) and, unlike C_V in pure water, remains constant ($C_{V,x} \cong 3.5$ J·mol^{-1}·K^{-1}) as the critical point is approaching, $\tau(x) \rightarrow 0$.

We are not aware of any $C_{V,x}$ measurements in dilute water + toluene mixtures; therefore, we cannot confirm or refute this prediction by direct comparison with experimental data. For this purpose more experimental mesurements in water + toluene mixtures are needed.

Acknowledgment

The authors are indebted to E. W. Lemmon and R. T. Jacobsen for providing us with their computer program for calculation of the thermodynamic properties of pure toluene prior to publication. M.A. thanks the Physical and Chemical Properties Division at the National Institute of Standards and Technology (NIST) for the opportunity to work as a Guest Researcher at NIST during the course of this research. The research in the Dagestan Scientific Center was supported by Grant RFBR-00-02-17856. The research in the Colorado School of Mines was supported by the U.S. Department of Energy, Office of Basic Energy Sciences, under Grant DE-FG03-95ER14568.

Nomenclature

A = molar Helmholtz free energy of the mixture
A_0 = critical amplitude in eq 26
$\tilde{A}$ = isomorphic molar free energy of the mixture
$\tilde{A}_0$ = background contribution
$\tilde{A}_i$ = system-dependent coefficients in eq 4 ($i = 1-4$)
$\tilde{a}$ = critical amplitude of the asymptotic term
b^2 = universal linear-model parameter
C_P = isobaric heat capacity
C_V = isochoric heat capacity
c = mass concentration
$\tilde{c}_i$ = critical amplitude of the nonasymptotic terms
$\tilde{d}_1$ = rectilinear diameter amplitude
e_i = universal constants in the scaled functions ($i = 0-5$)
G^0 = Gibbs energy
Gi = Ginzburg number
$\tilde{g}$ = inverse Ginzburg number
K_T = compressibility
$\tilde{k}$ = asymptotic critical amplitude of the coexistence curve
$k_i^{(j)}$ = mixture coefficients in eqs 14 and 15 ($j = 1$ and 2)
M_i = current mass of the water + toluene mixture
M_W = molecular weight
m = molality
m_w = mass of water
$\tilde{m}_i$ = system-dependent coefficients in eq 4 ($i = 1-4$)
P = pressure, MPa
P_c = critical pressure, MPa
P_i = mixture coefficients in eq 11
q = argument of the crossover function
R = gas constant
$\tilde{R}$ = crossover function
R_0 = resistance of the thermometer, Ω
r = parametric variable
T = temperature, K
T_c = critical temperature, K
T_i = mixture coefficients in eq 9
V = molar volume
$\bar{V}$ = partial molar volume
V_{TP} = piezometer volume
W = sound velocity
x = molar concentration
$\tilde{x}$ = isomorphic variable
Z_c = critical compressibility factor
Z_{cid} = "ideal" part of the critical compressibility factor
ΔZ_c = excess critical compressibility factor

Greek Letters

α = universal critical exponent
α_T = thermal expansion coefficient eq 17
β = universal critical exponent
β_P = pressure expansion coefficient in eq 17
γ = universal critical exponent
Δ = difference
$\Delta_i, \tilde{\Delta}_i$ = universal critical exponents ($i = 0-5$)
μ_i = chemical potentials of components ($i = 1$ and 2)
$\tilde{\mu}$ = chemical potential of mixture
Ψ_i = universal scaled functions ($i = 0-5$)
τ = reduced temperature difference
τ_α = dimensionless parameter in eq 26
ρ = molar density
ρ_c = critical density
ρ_i = mixture coefficients in eq 10
ϑ = parametric variable

Superscripts

cal = calculated
exp = experimental

Subscripts

0 = pure solvent
1 = pure solute
CRL = critical line
CXC = coexistence curve
c = critical
S = saturated
tot = total
w = water

Literature Cited

(1) Penniger, J. M. L. In *Supercritical Fluid Technology*; Penninger, J. M. L., Rodosz, M., McHugh, M. A., Krukonis, V. J., Eds.; Elsevier: New York, 1987; pp 309−329.

(2) Naragan, R.; Antol, M. J. In *Supercritical Fluid Science and Technology*; Joohnston, K. P., Penninger, J. M. L., Eds.; American Chemical Society: Washington, DC, 1989; pp 226−241.

(3) Modell, M.; Gaudet, G. G.; Simson, M.; Hong, G. T.; Bieman, K. Supercritical Water. *Solid Waste Manage.* **1982**, *26*, 30.

(4) Thomason, T. B.; Modell, M. Supercritical Water Destruction of Aqueous Wastes. *Hazard. Waste* **1984**, *1*, 453−462.

(5) Staszak, C. N.; Malinovski, K. C.; Killilea, W. R. The Pilot-Scale Demonstration of the MODAR Oxidation Process for the Destruction of Hazardous Organic Waste Materials. *Environ. Prog.* **1987**, *6*, 39−48.

(6) Barner, H. E.; Huang, C. Y.; Johnson, T.; Jacobs, G.; Martch, M. A. Supercritical Water Oxidation: An Emerging Technology. *J. Hazard. Mater.* **1992**, *32*, 1.

(7) Shaw, R. V.; Brill, N. B.; Clifford, A. A.; Eckert, C. A.; Franck, E. U. Supercritical Water: A Medium for Chemistry. *Chem. Eng. News* **1991**, *69*, 36.

(8) Eckert, C. A.; Ziger, D. H.; Johnston, K. P.; Ellison, T. K. The Use of Partial Molar Volume Data to Evaluate Equations of State for Supercritical Fluids Mixtures. *Fluid Phase Equilib.* **1983**, *14*, 167.

(9) Wu, R. S.; Lee, L. L.; Cochran, H. D. Structure of dilute Supercritical Solutions: Clustering of Solvent and Solute Molecules and the Thermodynamic Effects. *Ind. Eng. Chem. Res.* **1990**, *29*, 977.

(10) Petsche, I. B.; Debenedetti, P. G. Solute−Solvent Interactions in Infinitely Dilute Supercritical Mixtures: A Molecular Dynamics Investigation. *J. Chem. Phys.* **1989**, *91*, 7075.

(11) Gao, J. Supercritical Hydration of Organic Compounds. The Potential of Mean Force for Benzene Dimer in Supercritical Water. *J. Am. Chem. Soc.* **1993**, *115*, 6893.

(12) McGuigan, D. B.; Monson, P. A. Analysis of Infinite Dilution Partial Molar Volumes Using a Distribution Function Theory. *Fluid Phase Equilib.* **1990**, *57*, 227.

(13) Fernandez-Prini, R.; Japas, M. L. Critical Behavior of Fluid Binary Mixtures: Intermolecular Parameters and Thermodynamic Properties. *J. Phys. Chem.* **1992**, *96*, 5115.

(14) Kajimoto, O. Solvation in Supercritical Fluids: Its Effects on Energy Transfer and Chemical Reactions. *Chem. Rev.* **1990**, *90*, 355.

(15) Chialvo, A. A.; Cummings, P. T.; Yu, V. K. Solvation Effect on Kinetic Rate Constant of Reactions in Supercritical Solvents. *AIChE J.* **1998**, *44*, 667.

(16) Roberts, C. B.; Brennecke, J. F.; Chateauneu, J. E. Solvation Effects on Reactions of Triplet Benzophenone in Supercritical Fluids. *AIChE J.* **1995**, *41*, 1306.

(17) Reid, R. C.; Prausnitz, J. M.; Sherwood, T. K. *The properties of gases and liquids*, 3rd ed.; McGraw-Hill: New York, 1977.

(18) Walas, S. M. *Phase Equilibrium in Chemical Engineering*; Butterworth Publishers: Boston, 1985.

(19) Sengers, J. V.; Levelt Sengers, J. M. H. Thermodynamic behavior of fluids near the critical point. *Annu. Rev. Phys. Chem.* **1986**, *37*, 189−222.

(20) Anisimov, M. A.; Kiselev, S. B. In *Soviet Technology Review B*: *Thermal Physics*; Scheindlin, A. E., Fortov, V. E., Eds.; Harwood Academic: New York, 1992; Vol. 3, Part 2; pp 1−121.

(21) Fisher, M. Renormalization of Critical Exponents by Hidden Variables. *Phys. Rev. B* **1968**, *176*, 257−271.

(22) Griffiths, R. B.; Wheeler, J. C. Critical points in multicomponent system. *Phys. Rev. A* **1970**, *2*, 1047−1064.

(23) Saam, W. F. Thermodynamics of binary systems near the liquid−gas critical point. *Phys. Rev. A* **1970**, *2*, 1461−1466.

(24) Anisimov, M. A.; Voronel, A. V.; Gorodetskii, E. E. Isomorphism of Critical Phenomena. *Sov. Phys. JETP* **1971**, *33*, 605−611.

(25) Kiselev, S. B. Scaled Equation of State of Single-Component Liquids and Binary Solutions in the Critical Region. *High Temp.* **1988**, *26*, 337.

(26) Jin, G. X.; Tang, S.; Sengers, J. V. Global thermodynamic behavior of fluid mixtures in the critical region. *Phys. Rev. E* **1993**, *47*, 388−402.

(27) Povodyrev, A. A.; Jin, G. X.; Kiselev, S. B.; Sengers, J. V. Crossover Equation of State for the Thermodynamic Properties of MIxtures of Methane and Ethane in the Critical Region. *Int. J. Thermophys.* **1996**, *17*, 909−944.

(28) Kiselev, S. B.; Povodyrev, A. A. Crossover Behavior of Binary Solutions in the Critical Region. *High Temp.* **1996**, *34*, 621−639.

(29) Belyakov, M. Y.; Kiselev, S. B.; Rainwater, J. C. Cross Leung-Griffiths model and the phase behavior of dilute aqueous ionic solutions. *J. Chem. Phys.* **1997**, *107*, 3085−3097.

(30) Kiselev, S. B.; Belyakov, M. Y.; Rainwater, J. C. Crossover Leung-Griffiths model and the phase behavior of binary mixtures with and without chemical reaction. *Fluid Phase Equilib.* **1998**, *150*, 439−449.

(31) Kiselev, S. B.; Rainwater, J. C. Extended law of corresponding states and thermodynamic properties of binary mixtures in and beyond the critical region. *Fluid Phase Equilib.* **1997**, *141*, 129−154.

(32) Kiselev, S. B.; Rainwater, J. C. Enthalpies, excess volumes, and specific heats of critical and supercritical binary mixtures. *J. Chem. Phys.* **1998**, *109*, 643−657.

(33) Kiselev, S. B.; Abdulagatov, I. M.; Harvey, A. H. Equation of State and Thermodynamic Properties of Pure D_2O and D_2O + H_2O Mixtures in and beyond the Critical Region. *Int. J. Thermophys.* **1999**, *20*, 563−588.

(34) Van Konynenberg, P. H.; Scott, R. L. Critical lines and phase equilibria in binary van der Waals Mixtures. *Philos. Trans. R. Soc. London* **1980**, *298*, 495.

(35) Edison, T. A.; Anisimov, M. A.; Sengers, J. V. Critical scaling laws and excess Gibbs energy model. *Fluid Phase Equilib.* **1998**, *150−151*, 429−438.

(36) Cheng, H.; Anisimov, M. A.; Sengers, J. V. Prediction of thermodynamic and transport properties in the one-phase region of methane + *n*-hexane mixtures near their critical end points. *Fluid Phase Equilib.* **1997**, *128*, 67−96.

(37) Rainwater, J. C. A Nonclassical Model of a Type 2 Mixture with Vapor−Liquid, Liquid−liquid, and Three-Phase Equilibria. *Int. J. Thermophys.* **2000**, *21*, 719−737.

(38) Degrange, S. Ph.D., University Blaise Pascal, 1998.

(39) Kiselev, S. B. Universal crossover functions for the free energies of single-component and two-component fluids in their critical regions. *High Temp.* **1990**, *28*, 47−55.

(40) Kiselev, S. B.; Kostyukova, I. G.; Povodyrev, A. A. Universal Crossover Behavior of Fluids and Fluid Mixtures in the Critical Region. *Int. J. Thermophys.* **1991**, *12*, 877−895.

(41) Kiselev, S. B.; Sengers, J. V. An improved parametric crossover model for the thermodynamic properties of fluids in the critical region. *Int. J. Thermophys.* **1993**, *14*, 1−32.

(42) Kiselev, S. B. Prediction of the thermodynamic properties and the phase behavior of binary mixtures in the extended critical region. *Fluid Phase Equilib.* **1997**, *128*, 1−28.

(43) Leung, S. S.; Griffiths, R. B. Thermodynamic properties near the liquid−vapor critical line in mixturesof He3 and He4. *Phys. Rev. A* **1973**, *8*, 2670−2683.

(44) Landau, L. D.; Lifshitz, E. M. *Statistical Physics*; Pergamon Press: New York, 1980; Part 1.

(45) Patashinskii, A. Z.; Pokrovskii, V. L. *Fluctuation Theory of Phase Transitions*, 3rd ed.; Pergamon: New York, 1979.

(46) Anisimov, M. A.; Kiselev, S. B.; Sengers, J. V.; Tang, S. Crossover approach to global critical phenomena in fluids. *Physica A* **1992**, *188*, 487−525.

(47) Kiselev, S. B.; Rainwater, J. C.; Huber, M. L. Binary mixtures in and beyond the critical region: thermodynamic properties. *Fluid Phase Equilib.* **1998**, *150−151*, 469−478.

(48) Kiselev, S. B.; Huber, M. L. Thermodynamic properties of R32 + R134a and R125 + R32 mixtures in and beyond the critical region. *Int. J. Refrig.* **1998**, *21*, 64−76.

(49) Kiselev, S. B.; Povodyrev, A. A. An Isomorphic Generalization of the Law of Corresponding States for Binary Mixtures. *Fluid Phase Equilib.* **1992**, *79*, 33−47.

(50) Albert, H. J.; Gates, J. A.; Wood, R. H.; Grolier, J.-P. E. Density of Toluene, of Butanol and of Their Binary Mixtures from 298 to 400 K and from 0.5 to 20 MPa. *Fluid Phase Equilib.* **1985**, *20*, 321.

(51) Dymond, J. H.; Malhorta, R.; Isdale, J. D.; Glen, N. F. (*P*, *r*, *T*) of *n*-Heptane, Toluene, and Oct-1-ene in the Range 298 to 373 K and 0.1 to 400 MPa and Representation by the Tait Equation. *J. Chem. Thermodyn.* **1988**, *20*, 603.

(52) Dymond, J. H.; Awan, M. A.; Glen, N. F.; Isdale, J. D. Transport Properties of Nonelectrolyte Liquid Mixtures. VIII. Viscosity Coefficients for Toluene and for Three Mixtures of Toluene + *n*-Hexane from 25 to 100 °C at Pressures up to 500 MPa. *Int. J. Thermophys.* **1991**, *12*, 275.

(53) Kashiwagi, H.; Kashimoto, T.; Tanaka, Y.; Kubota, H.; Makita, T. Thermal Conductivity and Density of Toluene in the Temperature Range 273−373 K at Pressures up to 250 MPa. *Int. J. Thermophys.* **1981**, *3*, 201.

(54) Marcos, D. H.; Lindley, D. D.; Wilson, K. S.; Kay, W. B.; Hershey, H. C. A (*P*, *V*, *T*) Study of Tetramethylslilane, Hexamethyldisiloxane, Octamethyltrisiloxane, and Toluene from 423 to 523 K in the Vapor Phase. *J. Chem. Thermodyn.* **1983**, *15*, 1003.

(55) Muringer, M. J. P.; Trappeniers, N. J.; Biswas, S. N. The Effect of Pressure on the Sound Velocity and Density of Toluene and *n*-Heptane up to 2600 bar. *Phys. Chem. Liq.* **1985**, *14*, 273.

(56) Takagi, T.; Teranish, H. Ultrasonic Speeds and Densities of Benzene and Toluene under High Pressures. *Zairyo* **1984**, *33*, 134.

(57) Watanabe, N.; Yokoyama, C.; Takahashi, S. *PVT* Relationship of Gaseous Toluene at Temperatures from 500 to 600 K. *Kagaku Kogaku Ronbunshu* **1988**, *14*, 525.

(58) Magee, J. W.; Bruno, T. J. Isochoric (*P*, *ρ*, *T*) Measurements for Liquid Toluene from 180 to 400 K at Pressures to 35 MPa. *J. Chem. Eng. Data* **1996**, *41*, 900.

(59) Straty, G. C.; Ball, M. J.; Bruno, T. J. *PVT* of Toluene at Temperatures to 673 K. *J. Chem. Eng. Data* **1988**, *33*, 115.

(60) Akhundov, T. S.; Abdullaev, F. G. Specific Volumes of Toluene in the Critical Region. *Izv. Vyssh. Uchebn. Zaved., Neft Gas (Russian)* **1974**, *1*, 62.

(61) Pöhler, H.; Kiran, E. Volumetric Properties of Carbon Dioxide + Toluene at High Pressures. *J. Chem. Eng. Data* **1996**, *41*, 482.

(62) Franck, E. U.; Kerschbaum, S.; Wiegand, G. The Density of Toluene at High Pressures to 673 K and 300 MPa. *Ber. Bunsen-Ges. Phys. Chem.* **1998**, *102*, 1794.

(63) Akhundov, T. S.; Abdullaev, F. G. In *Thermophysical Properties of Liquids*; Novikov, I. I., Ed.; Nauka: Moscow, 1970.

(64) Polikhronidi, N. G.; Abdulagatov, I. M.; Magee, J. W.; Batyrova, R. G. Isochoric Heat Capacity for Toluene Near Phase Transitions and the Critical Point. *J. Chem. Eng. Data* **2001**, in press.

(65) Mamedov, A. M.; Akhundov, T. S. Thermodynamic Properties of Gases and Liquids. *Aromatic Hydrocarbons (Russian)*; GSSSD: Moscow, 1978.

(66) Zotov, V. V.; Kireev, B. N.; Neruchev, Y. A. Study of the Equilibria Properties of Hydrocarbons on the Coexistence Curve Using Acoustic Method. *Prikl. Mekh. Tekh. Fiz. (Russian)* **1975**, *2*, 162.

(67) Okhotin, V. S.; Razumeichenko, L. A.; Kas'yanov, Y. I. In *Thermophysical Properties of Substances and Materials (Russian)*; GSSSD: Moscow, 1991; Vol. 30, p 20.

(68) Hales, J. L.; Townsend, R. Liquid Densities from 293 to 490 K of Nine Aromatic Hydrocarbons. *J. Chem. Thermodyn.* **1972**, *4*, 763.

(69) Chirico, R. D.; Steele, W. V. Reconciliation of Calorimetrically and Spectroscopically Derived Thermodynamic Properties at Pressures Greater Than 0.1 MPa for Benzene and Methylbenzene: The Importance of the Third Virial Coefficient. *Ind. Eng. Chem. Res.* **1994**, *33*, 157.

(70) Rudenko, A. P.; Sperkach, V. S.; Timoshenko, A. N.; Yagupol'skii, L. M. The Elastic Properties of Trifluoromethylbenzene along the Equilibrium Curve. *Russ. J. Phys. Chem.* **1981**, *55*, 1054.

(71) Shraiber, L. S.; Pechenyuk, N. G. The Temperature Dependency of Density of Some Organic Liquids. *Russ. J. Phys. Chem.* **1965**, *39*, 429.

(72) Francis, A. W. Pressure−Temperature−Liquid Density Relations of Pure Hydrocarbons. *Ind. Eng. Chem.* **1957**, *49*, 1779.

(73) Goodwin, R. D. Toluene Thermophysical Properties from 178 to 800 K at Pressures to 1000 bar. *J. Phys. Chem. Ref. Data* **1989**, *18*, 1565.

(74) Krase, N. W.; Goodman, J. B. Vapor Pressure of Toluene up to the Critical Temperature. *Ind. Eng. Chem.* **1930**, *22*, 13.

(75) Ambrose, D.; Broderick, B. E.; Townsend, R. The Vapor Pressures above the Normal Boiling Point and the Critical Pressures of Some Aromatic Hydrocarbons. *J. Chem. Soc. A* **1967**, 633.

(76) Ambrose, D. Vapor-Pressure of Some Aromatic Hydrocarbons. *J. Chem. Thermodyn.* **1987**, *19*, 1007.

(77) Griswold, D. A.; Andres, D.; Klein, V. A. Determination of High-Pressure Vapor−Liquid Equilibria. The Vapor−Liquid Equilibrium of Benzene−Toluene. *Trans. Am. Inst. Chem. Eng.* **1943**, *39*, 223.

(78) Mamedov, A. M.; Akhundov, T. S.; Imanov, S. Y.; Abdullaev, F. G.; Asadullaeva, N. N. In *Thermophysical Properties of Substances and Materials (Russian)*; Rabinovich, V. A., Ed.; GSSSD: Moscow, 1973; Vol. 6, p 110.

(79) Polt, A.; Platzer, B.; Maurer, G. Parameter of the Thermal Equation of State by Bender for 14 Polyatomic Pure Substances. *Chem. Tech.* **1992**, *6*, 216.

(80) Lemmon, E. W.; Jacobsen, R. T. (NIST, Boulder, CO). Private communication, 2001.

(81) Chandler, K.; Eason, B.; Liotta, C. L.; Eckert, C. A. Phase Equilibria for Binary Aqueous Systems from a Near-Critical Water Reaction Apparatus. *Ind. Eng. Chem. Res.* **1998**, *37*, 3515.

(82) Anderson, F. E.; Prausnitz, J. M. Mutual Solubilities and Vapor Pressures for Binary and Ternary Aqueous Systems Containing Benzene, Toluene, *m*-Xylene, Thiophene and Pyridine in the Region 100−200 °C. *Fluid Phase Equilib.* **1986**, *32*, 63.

(83) Roof, J. G. Three-Phase Critical Point in Hydrocarbon−Water Systems. *J. Chem. Eng. Data* **1970**, *15*, 301.

(84) Connolly, J. F. Solubility of Hydrocarbons in Water Near the Critical Solution Temperatures. *J. Chem. Eng. Data* **1966**, *14*, 13.

(85) Chen, H.; Wagner, J. An Efficient and Reliable Gas Chromatographic Method for Measuring Liquid−Liquid Mutual Solubilities in Alkylbenzene + Water Mixtures; Toluene + Water from 303 to 373 K. *J. Chem. Eng. Data* **1994**, *39*, 475.

(86) Alwani, Z. Ph.D., Universitäit Karlsruhe, 1969.

(87) Alwani, Z.; Schneider, G. M. Phase equilibria, critical phenomena and PVT data in binary mixtures of water with aromatic hydrocarbons from 420 °C and 2200 bar. *Ber. Bunsen-Ges. Physik. Chem.* **1967**, *73*, 294.

(88) Haruki, M.; Yahiro, Y.; Higashi, H.; Arai, Y. Correlation of Phase Equilibria for Water + Hydrocarbon Systems at High Temperatures and Pressures by Cubic Equation of State. *J. Chem. Eng. Jpn.* **1999**, *32*, 535.

(89) Haruki, M.; Iwai, Y.; Nagao, S.; Yahiro, Y.; Arai, Y. Measurements and Correlation of Phase Equilibria for Water + Hydrocarbon Systems Near the Critical temperature and Pressure of Water. *Ind. Eng. Chem. Res.* **2000**, *39*, 4516.

(90) Majer, V.; Degrange, S.; Sedlbauer, J. Temperature Correlation of Partial Molar Volumes of Aqueous Hydrocarbons at Infinite Dilution: Test of Equations. *Fluid Phase Equilib.* **1999**, *158*, 419.

(91) Abdulagatov, I. M.; Bazaev, A. R.; Ramazanova, A. E. *PVTx* Measurements of Aqueous Mixtures at Supercritical Conditions. *Int. J. Thermophys.* **1993**, *14*, 231.

(92) Abdulagatov, I. M.; Bazaev, A. R.; Bazaev, E. A.; Saidakhmedova, M. B.; Ramazanova, A. E. *PVTx* Measurements and Partial Molar Volumes for Water−Hydrocarbon Mixtures in the Near-Critical and Supercritical Conditions. *Fluid Phase Equilib.* **1998**, *150*, 537.

(93) Abdulagatov, I. M.; Bazaev, E. R.; Bazaev, A. R.; Rabezkii, M. G. *PVTx* Measurements for Water + *n*-Hexane Mixtures in the Near-Critical and Supercritical Regions. *J. Supercrit. Fluids* **2001**, *10*, 149.

(94) Wagner, W.; Pruss, A. New International Formulation for the Thermodynamic Properties of Ordinary Water Substance for General and Scientific Use. (private communication).

(95) Harvey, A. H.; Peskin, A. P.; Klein, S. A. NIST/ASME Steam Properties, NIST Standard Reference Database 10, Version 2.2, 2000.

(96) Kiselev, S. B.; Friend, D. G. Revision of a multiparameter equation of state to improve the representation in the critical region: application to water. *Fluid Phase Equilib.* **1999**, *155*, 33−55.

(97) Akhundov, T. S.; Eksaev, R. A.; Sultanov, C. I. Heat Capacity (Cp) of Toluene. Experimental Apparatus. *Thermophys. Prop. Subst. Mater.* **1973**, *7*, 84.

(98) Abdulagatov, I. M.; Magee, J. W.; Kiselev, S. B.; Friend, D. G. *A Critical Assessment of Experimental Data for Heat Capacity at Constant Volume of Water and Steam*; NISTIR: Washington, DC, 2001.

(99) Nefedov, S. N.; Filippov, L. P. Experimental Study of Heat Capacity, Thermal Diffusivity, and Thermal Activity of Toluene. *Izv. Vyssh. Uchebn. Zaved., Neft Gas (Russian)* **1980**, *23*, 51.

(100) Pankevich, G. M.; Zotov, V. V. In *Nauchnye Trudy Kurskogo Pedagogicheskogo Instituta (Russian)*; Kursk Pedagogical Institute: Kursk, 1976; Vol. 81, p 91.

(101) Zotov, V. V. In *Uchenye Zapiski Kurskogo Gosudarstvennyi Pedagogicheskii Institut (Russian)*; Kursk Pedagogikal Institute: Kursk, 1969; Vol. 54, p 63.

(102) Chang, R. F.; Levelt Sengers, J. M. H. Behavior of Dilute Mixtures Near the Solvent's Critical Point. *J. Phys. Chem.* **1986**, *90*, 5921.

(103) Chang, R. F.; Morrison, G.; Levelt Sengers, J. M. H. The Critical Dilemma of Dilute Mixtures. *J. Phys. Chem.* **1984**, *88*, 3389.

(104) O'Connell, J. P.; Sharygin, A. V.; Wood, R. H. Infinite Dilution Partial Molar Volumes of Aqueous Solutions over Wide Range Conditions. *Ind. Eng. Chem. Res.* **1996**, *35*, 2808.

(105) Chimowitz, E. H.; Afrane, G. Classical, Non-Classical Critical Divergences and Partial Molar Properties from Adsorption Measurements in Near-Critical Mixtures. *Fluid Phase Equilib.* **1996**, *120*, 167.

(106) Wheeler, J. C. Behavior of a Solute Near the Critical Point of an Almost Pure Solvent. *Ber. Bunsen-Ges. Phys. Chem.* **1972**, *76*, 308.

(107) Khazanova, N. E.; Sominskaya, E. E. Partial Molar Volumes in the Etahane−Carbon dioxide Systems Near the Critical Points of the Pure Components. *Russ. J. Phys. Chem.* **1971**, *45*, 1485.

(108) van Wasen, U.; Swaid, I.; Schneider, G. M. *Angew. Chem., Int. Ed. Engl.* **1980**, *19*, 575.

(109) Levelt Sengers, J. M. H. Solubility Near the Solvent's Critical Point. *J. Supercrit. Fluids* **1991**, *4*, 215.

(110) Harvey, A. H.; Levelt Sengers, J. M. H. Unified Description of Infinite-Dilution Thermodynamic Properties for Aqueous Solutions. *J. Phys. Chem.* **1991**, *95*, 932.

(111) Harvey, A. H.; Levelt Sengers, J. M. H. Correlation of Aqueous Henry's Constant from 0 °C to the Critical Point. *AIChE J.* **1990**, *36*, 539.

(112) Harvey, A. H. Supercritical Solubility of Solids from Near-Critical Dilute-Mixture Theory. *J. Phys. Chem.* **1990**, *94*, 8403.

(113) Furuya, T.; Teja, A. S. Krichevskii Parameter and Solubility of Heavy *n*-Alkanes in Supercritical Carbon Dioxide. *Ind. Eng. Chem. Res.* **2000**, *39*, 4828.

(114) Japas, M. L.; Levelt Sengers, J. M. H. Gas Solubility and Henry's Law Near the Solvent Critical Point. *AIChE J.* **1989**, *35*, 705.

(115) Levelt Sengers, J. M. H.; Morrison, G.; Nielson, G.; Chang, R. F.; Everhart, C. M. Thermodynamic Behavior of Supercritical Fluid Mixtures. *Int. J. Thermophys.* **1986**, *7*, 231.

(116) Levelt Sengers, J. M. H. In *Supercritical Fluids*: *Fundamentals for Applications*; Kiran, E., Levelt Sengers, J. M. H., Eds.; Kluwer: Dordrecht, The Netherlands, 1994; pp 13−37.

(117) Japas, M. L.; Alvarez, J. L.; Gutkovski, K.; Fernandez-Prini, R. Determination of the Krichevskii Function in the Near-Critical Dilute Solutions of I_2(s) and CHI_3(s). *J. Chem. Thermodyn.* **1998**, *30*, 1603.

(118) Chialvo, A. A.; Cummings, P. T. Solute-Induced Effects on the Supercritical and Thermodynamics of Infinitely Dilute Mixtures. *AIChE J.* **1994**, *40*, 1558.

(119) Chialvo, A. A.; Cummings, P. T. Comments on Near Critical Phase Behavior of Dilute Mixtures. *Mol. Phys.* **1995**, *84*, 41.

(120) Cummings, P. T.; Chialvo, A. A. Molecular Simulation Study of Solvation Structure in Supercritical Aqueous Solutions. *Chem. Eng. Sci.* **1994**, *49*, 2735.

(121) Debenedetti, P. G.; Kumar, S. K. The Molecular Basis of Temperature Effects in Supercritical Extraction. *AIChE J.* **1984**, *34*, 645.

(122) Debenedetti, P. G.; Mohamed, R. S. Attractive, Weakly Attractive, and Repulsive Near-Critical Systems. *J. Chem. Phys.* **1989**, *90*, 4528.

(123) Krichevskii, I. R. Thermodynamics of Critical Phenomena in Infinitely Dilute Binary Solutions. *Russ. J. Phys. Chem.* **1967**, *41*, 1332.

(124) Rozen, A. M. The Unusual Properties of Solutions in the Vicinity of the Critical Point of the Solvent. *Russ. J. Phys. Chem.* **1976**, *50*, 837.

(125) Levelt Sengers, J. M. H. In *Supercritical Fluid Technology*; Ely, J. F., Bruno, T. J., Eds.; CRC Press: Boca Raton, FL, 1991; p 1.

(126) Gude, M. T.; Teja, A. S. The Critical Properties of Dilute *n*-Alkane Mixtures. *Fluid Phase Equilib.* **1993**, *83*, 139.

(127) Gude, M. T.; Teja, A. S. The Near-Critical Phase Behavior of Dilute Mixtures. *Mol. Phys.* **1994**, *81*, 599.

(128) Levelt Sengers, J. H. M. *Physical Chemistry of Aqueous Systems.* In *Proceedings of the 12th International Conference on the Properties of Water and Steam*; White, H. J., Sengers, J. V., Neumann, D. B., Bellows, J. C., Eds.; Begell House: Orlando, FL, 1995; p A143.

(129) Plyasunov, A. V.; Shock, E. L. Estimation of the Krichevskii Parameter for Aqueous Nonelectrolytes. *J. Supercrit. Fluids* **2001**, *20*, 91.

(130) Kiselev, S. B.; Friend, D. G. Cubic crossover equation of state for mixtures. *Fluid Phase Equilib.* **1999**, *162*, 51−82.

(131) Bazaev, A. R.; Abdulagatov, I. M.; Magee, J. W.; M. G., R.; Bazaev, E. A. *PVT* Measurements for Toluene in the Near-Critical and Supercritical Regions. *J. Chem. Eng. Data* **2001**, in press.

Received for review April 2, 2001
Revised manuscript received May 29, 2001
Accepted June 4, 2001

IE010307M